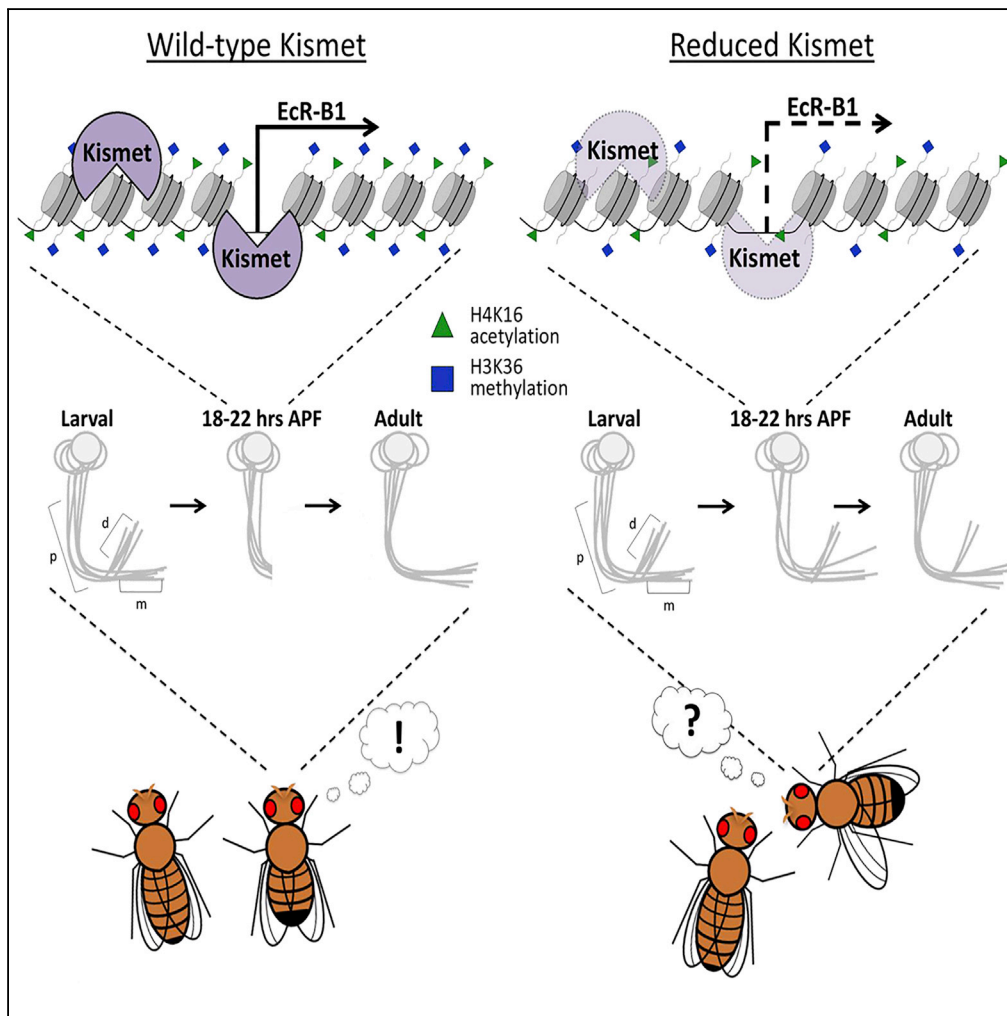**Article**

The *Drosophila* Chromodomain Protein Kismet Activates Steroid Hormone Receptor Transcription to Govern Axon Pruning and Memory *In Vivo*

Nina K. Latcheva,
Jennifer M.
Viveiros, Daniel R.
Marenda

daniel.marenda@drexel.edu

HIGHLIGHTS

Kismet activates *ecr-b1* transcription to initiate developmental axon pruning

Kismet promotes H3K36 di- and tri-methylation and H4K16 acetylation

Axon pruning and memory defects of Kismet mutants are rescued by HDAC inhibition

Article

The *Drosophila* Chromodomain Protein Kismet Activates Steroid Hormone Receptor Transcription to Govern Axon Pruning and Memory *In Vivo*

Nina K. Latcheva,[1,2] Jennifer M. Viveiros,[1] and Daniel R. Marenda[1,2,3,4,*]

SUMMARY

Axon pruning is critical for sculpting precise neural circuits. Although axon pruning has been described in the literature for decades, relatively little is known about the molecular and cellular mechanisms that govern axon pruning *in vivo*. Here, we show that the epigenetic reader Kismet (Kis) is required for developmental axon pruning in *Drosophila* mushroom bodies. Kis binds to cis-regulatory elements of the steroid hormone receptor *ecdysone receptor* (*ecr*) gene and is necessary for activating expression of EcR-B1. Kis promotes the active H3K36 di- and tri-methylation and H4K16 acetylation histone marks at the *ecr* locus. We show that transgenic EcR-B1 can rescue axon pruning and memory defects associated with loss of Kis and that the histone deacetylase inhibitor SAHA also rescues these phenotypes. EcR protein abundance is the cell-autonomous, rate-limiting step required to initiate axon pruning in *Drosophila*, and our data suggest this step is under the epigenetic control of Kis.

INTRODUCTION

The elimination and refinement of synaptic connections is an integral part of normal development in vertebrates and invertebrates alike. Early in the developing nervous system, periods of progressive growth result in an overelaboration of synaptic connections onto a target. Inappropriate synapses then need to be eliminated to establish functional organization of the neuronal circuitry (Tau and Peterson, 2010). The pruning of these exuberant connections can occur on a small scale, as with dendritic remodeling, or on a large scale, such as with axon retraction and degeneration, with each type occurring through distinct molecular mechanisms (Low and Cheng, 2006). Precise control of axon pruning is critical for proper nervous system function, as defects in pruning have been well documented to lead to developmental neurological and psychiatric disorders (Tau and Peterson, 2010). Despite its vital role, relatively little is known about the mechanisms that govern axon pruning *in vivo*. What is well known about this process is that it requires tight regulation of gene expression to execute the necessary signaling pathways in a temporal and tissue-specific manner (Awasaki et al., 2011; Yu and Schuldiner, 2014). Epigenetic regulation is key to orchestrating precise gene expression programs for many tightly controlled processes in the body. However, its involvement in axon pruning is still unclear.

Holometabolous insects provide an attractive model for studying axon pruning as their nervous system undergoes extensive reorganization during metamorphosis (Levine et al., 1995; Truman, 1990). In *Drosophila melanogaster*, the larval neuronal circuitry is eliminated to make way for adult-specific circuitry that governs adult-specific behaviors. The most notable changes occur in the learning and memory processing center of the fly brain known as the mushroom bodies (MBs) (Connolly et al., 1996; Ferveur et al., 1995; Heisenberg et al., 1985; McBride et al., 1999). The MBs are bilaterally symmetrical structures in the central brain that are composed of ~2,500 Kenyon cells divided into five populations of neurons: gamma, alpha, beta, alpha prime, and beta prime (Ito et al., 1997; Lee et al., 1999). Each Kenyon cell has dendrites, which extend into a structure called the calyx, as well as densely packed axons that make up the MB peduncle. From the peduncle, the axons then divide to form two separate lobes that extend into the dorsal and medial direction. The gamma neurons are generated first in development and initially during the larval stages extend bifurcated axons in the dorsal and medial lobes (Ito et al., 1997; Lee et al., 1999; Spindler and Hartenstein, 2010; Technau and Heisenberg, 1982). During metamorphosis, however, the gamma neuron axons are selectively pruned back to the peduncle to eliminate the bifurcation. At approximately 18–22 h after puparium formation (APF), the gamma neuron axons begin to re-extend new axons only into the medial lobe. This stereotypical developmental pruning of the gamma neurons has been shown

[1]Department of Biology, Drexel University, 3141 Chestnut St., Philadelphia, PA 19104, USA

[2]Program in Molecular and Cellular Biology and Genetics, Drexel University College of Medicine, Philadelphia, PA, USA

[3]Department of Neurobiology and Anatomy, Drexel University College of Medicine, Philadelphia, PA, USA

[4]Lead Contact

*Correspondence: daniel.marenda@drexel.edu

https://doi.org/10.1016/j.isci.2019.05.021

to be initiated by the steroid hormone 20-hydroxyecdysone (ecdysone) (Awasaki et al., 2011; Lee et al., 2000; Zheng et al., 2003).

Ecdysone is most well known as the major molting hormone for its role in initiating each of the developmental transitions in arthropods (Handler, 1982). In *Drosophila*, ecdysone is released in large quantities by the prothoracic gland before each of the larval molts and pupation. The ligand is then able to enter the cytoplasm of target cells where it can bind to the Ecdysone Receptor (EcR). The binding of ecdysone to EcR stabilizes its interaction with its dimerization partner Ultraspiracle (Thummel, 2002; Yamanaka et al., 2013). The stable heterodimer enters the nucleus and activates transcription of a small subset of regulatory target genes known as immediate-early genes, which possess ecdysone response elements in the promotor regions (Ashburner, 1974; Ashburner et al., 1974; Thummel, 2002; Yamanaka et al., 2013). The specific responses different tissues have to induction of the ecdysone signaling cascade can be correlated to the three different EcR isoforms expressed in *Drosophila*: EcR-A, EcR-B1, and EcR-B2 (Talbot et al., 1993; Truman, 1990; Truman et al., 1994). The gamma neurons of the MBs in particular express EcR-B1, which has been shown to be a rate-limiting and cell-autonomous step required for the developmental pruning of axons during metamorphosis (Lee et al., 2000). In addition, EcR-B1 and functional gamma neurons in adult flies were shown to be required for short-term memory and the formation of courtship-associated long-term memory (Boulanger and Dura, 2015; Ishimoto et al., 2009; Redt-Clouet et al., 2012).

Our laboratory previously identified the chromodomain protein Kismet (Kis) as necessary for proper developmental axon pruning in the *Drosophila* MB neurons, although the mechanism by which Kis accomplished this was unknown (Melicharek et al., 2010). Kis is the *Drosophila* ortholog of the mammalian chromatin ATPase chromodomain helicase DNA-binding protein 7 (CHD7), a chromatin "reader" that is thought to play a role in chromatin remodeling by binding to methylated histone tails (Layman et al., 2010). In humans, heterozygous mutations in *CHD7* cause CHARGE syndrome (Vissers et al., 2004), an autosomal dominant neurodevelopmental disorder.

Here, we investigated the role of Kis in the developmental axon pruning of the *Drosophila* MB neurons. We determined that the loss of Kis in the MBs results in pruning defects during metamorphosis, which persist into adulthood and are due to a decrease in expression of *ecr-b1*. We show that endogenous Kis is enriched at a previously identified region of the genome shown to be important for *ecr* gene expression and that Kis binds to and is required to promote transcription from at least one cis-regulatory enhancer site in MB neurons. Furthermore, loss of Kis leads to a decrease in the histone marks H3K36 di- and tri-methylation (H3K36me2 and H3K36me3, respectively), which have been associated with actively transcribed genes in flies. Additionally, loss of Kis results in a striking loss of H4K16 acetylation (H4K16ac). Adult flies with Kis specifically decreased in the MB neurons display a loss of immediate recall memory, which is rescued by transgenic expression of EcR-B1. Finally, we show that pharmacological intervention via the general histone deacetylase (HDAC) inhibitor suberoylanilide hydroxamic acid (SAHA) can rescue the decrease in *ecr-b1* mRNA, axon pruning, and memory defects associated with decreased Kis in MB neurons. Taken together, these data show that Kis-mediated regulation of *ecr-b1* is required for proper developmental axon pruning *in vivo* by mediating the epigenetic marks H3K36me2, H3K36me3, and H4K16ac. These findings suggest that the rate-limiting step required to initiate axon pruning (*ecr-b1* expression) is under the epigenetic control of Kis.

RESULTS

Kismet Is Required for MB Pruning

We have previously shown that Kismet protein is widely expressed throughout the larval brain, including in the MB neurons (Melicharek et al., 2010). To characterize the pruning defects previously observed in *kis* mutant MB neurons, we utilized the mosaic analysis with a repressible cell marker (MARCM) system to generate homozygous mutant neuroblast clones tagged with a membrane-bound GFP (*UAS:mCD8-GFP*) using the *201y-Gal4* driver (Lee and Luo, 1999; Melicharek et al., 2010; Schuldiner et al., 2008; Yang et al., 1995). To quantify the pruning defects, we measured dorsal, medial, and total surface area of the MB lobes in pupal brains 18–22 h APF. This developmental window is standard in the field and has been extensively used because of the stereotypical timing in which axon pruning occurs in this model (Boulanger et al., 2011; Lai et al., 2016; Lee et al., 1999, 2000). At this time point, the MB lobes are mostly eliminated in control animals leaving only the peduncle (Figures 1A and 1E). In agreement with our previous work, the MB clones of the null mutant *kis^LM27* (Melicharek et al., 2008), MB clones had significantly larger medial and
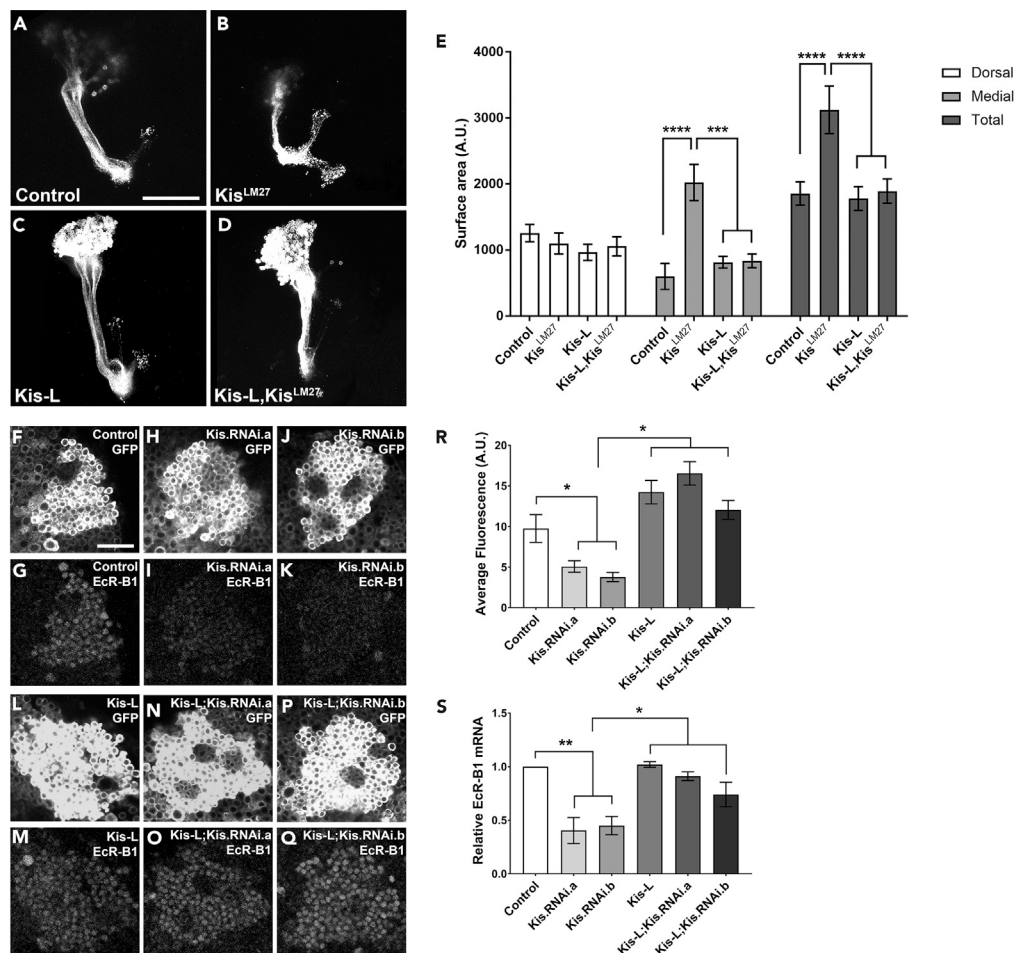
Figure 1. Kis Is Required for Developmental Axon Pruning and EcR Expression

(A–D) Representative images of MARCM-generated MB clones expressing membrane-bound GFP using the *201y-Gal4* driver 18–22 h APF. (A) control (w^{1118}; FRT40A), (B) kis null mutant (Kis^{LM27}, *FRT 40A*), (C) Kis overexpression (*UAS:Kis-L,FRT40A*), and (D) Kis rescue (*UAS:Kis-L,Kis^{LM27},FRT40A*).

(E) Quantification of dorsal, medial, and total MB lobe surface areas in MARCM animals (from left to right, n = 12, 11, 10, 12 MBs).

(F–Q) Representative images of pupal Kenyon cells using the *elav-Gal4,UAS:mCD8-GFP* driver 18–22 h APF. (F) control (w^{1118}) membrane bound GFP, (G) control (w^{1118}) EcR-B1 protein staining, Kis knockdowns: (H) GFP and (I) EcR-B1 in *UAS:Kis.RNAi.a* and (J) GFP and (K) EcR-B1 in *UAS:Kis.RNAi.b*. (L) Kis overexpression (*UAS:Kis-L*) GFP, and (M) EcR-B1 protein staining and Kis rescues: (N) GFP and (O) EcR-B1 in *UAS:Kis-L; UAS:Kis.RNAi.a*, and (P) GFP and (Q) EcR-B1 in *UAS:Kis-L,UAS:Kis.RNAi.b*.

(R) Quantification of α-EcR-B1 fluorescence intensity within pupal Kenyon cells (from left to right, n = 10, 10, 10, 10, 7, 10 MBs).

(S) Abundance of *ecr-b1* mRNA isolated from pupal heads analyzed by RT-qPCR using the *elav-Gal4* driver (number of biological replicates from left to right, 3, 3, 4, 3, 3, 3; 10 heads/biological replicate).

Scale bars: 10 μm in (A) and 20 μm in (F). Statistical significance is represented by * = $p < 0.05$, ** = $p < 0.01$, *** = $p < 0.001$, and **** = $p < 0.0001$. Error bars represent the SEM.

total lobe surface areas compared with control MB clones, indicative of unpruned axons (Figures 1A, 1B, and 1E) (Melicharek et al., 2010).

To expand upon our previous results, and to verify that loss of Kis was responsible for the MB pruning defect we observed, we expressed the wild-type Kis-L protein isoform (full length) in *kis^{LM27}* mutant MB clones. MB clones expressing Kis-L in the *kis^{LM27}* mutant background showed a significant reduction of the medial and total lobe areas (Figures 1D and 1E), suggesting the pruning defect is in fact due to loss of Kis protein function. Overexpression of Kis-L alone did not have an effect on lobe surface area compared with control MBs (Figures 1C and 1E). To verify the pruning defects we observed with the MARCM analysis,

we also utilized a second knockdown system: RNA interference (RNAi)-mediated knockdown of Kis with two separate previously validated RNAi constructs (Melicharek et al., 2010). Expression of Kis-L using the neuronal *elav-Gal4* driver produces nearly 3-fold the normal amount of *kis* mRNA (Figure S1). Additionally, expression of *Kis-L* in conjunction with either *Kis.RNAi.a* or *Kis.RNAi.b* significantly reduced *kis* mRNA levels compared with *Kis-L* alone (Figure S1), which would compensate (at least partially) the loss of Kismet knockdown provided by Kismet RNAi. Pan-neural knockdown of Kis using the *elav-Gal4,UAS:mCD8-GFP* driver showed a significant increase in the medial and total lobe surface areas compared with outcross controls (Figure S2). Similar to the MARCM analysis, pan-neural expression of Kis-L in the knockdown genetic backgrounds was able to significantly rescue the medial and total surface area levels (Figure S2). Taken together, these data validate and expand upon our previous findings and show that Kis is required for the developmental axon pruning of MB gamma neurons during metamorphosis.

Kismet Promotes EcR-B1 Protein and mRNA Expression

Expression of the steroid hormone receptor EcR-B1 is the first step in the developmental axon pruning of the MB neurons, and loss of EcR-B1 function produces defects in pruning similar to what we observe with decreased Kis function (Lee et al., 2000). Therefore, we sought to determine if Kis affects expression of EcR-B1. Pan-neural knockdown of Kis using the *elav-Gal4,UAS:mCD8-GFP* driver showed a significant decrease in EcR-B1 immunofluorescence in the MB Kenyon cells compared with those of control MBs at 18–22 h APF (Figures 1F–1K and 1R). Analysis of EcR-B1 protein staining during late third instar larval stage, when the ecdysone pulse is the highest, also reveals that MB Kenyon cells had a significant decrease of immunofluorescence levels upon loss of Kis (Figure S3) (Thummel, 2002). In support of these results, mRNA levels of *ecr-b1* were significantly reduced in pupal brains with pan-neural decreased expression of Kis as shown by RT-qPCR (Figure 1S). Additionally, replacement of Kis-L protein in the Kis knockdown background successfully rescued both decreased *ecr-b1* mRNA and EcR-B1 protein levels (Figures 1L–1S). Importantly, even though the *Kis-L* construct produces an overexpression of *kis* mRNA (Figure S1), this does not lead to a concomitant increase of EcR-B1 protein or mRNA levels outside of normal range (Figures 1R and 1S). This may be indicative of an upper limit to Kis's ability to promote EcR-B1 expression. Taken together, these data suggest that Kis is required to regulate EcR-B1 levels within MB neurons.

Kismet Binds *Ecr* Locus *In Vivo*

Given that Kis is an epigenetic chromatin reader, we theorized that it may be affecting *ecr-b1* mRNA and EcR-B1 protein levels by promoting transcription. To begin testing this hypothesis, we performed chromatin immunoprecipitation (ChIP) followed by qPCR using chromatin isolated from third instar larval brains to analyze Kis occupancy at the *ecr* locus. We probed three cis-regulatory element sites between 7 and 33 kb upstream of the *ecr-b* transcription start site (TSS) (Figure 2A). We chose this genomic region for analysis as previous work showed that multiple transcription factor binding sites important for *ecr-b1* expression are present in this area (Figure 2A) (Boulanger et al., 2011). We utilized a Kis-eGFP protein trap animal previously described to express an enhanced Green Fluorescent Protein (eGFP) tagged version of the endogenous Kis protein (Buszczak et al., 2007; Ghosh et al., 2014). Importantly, the Kis-eGFP protein did not affect protein localization or function compared with wild-type Kis (Ghosh et al., 2014), and *UAS:Kis.RNAi.a* can successfully knock down the eGFP-tagged Kis protein and *kis-eGFP* mRNA (Figure S4). The *forkhead* (*fkh*) TSS served as a positive control, as it was previously reported to be bound by endogenous Kis (Srinivasan et al., 2008). Additionally, we used the *dynamin* homolog *shibire* (*shi*) as a negative control, since we had previously shown via microarray analysis that loss of Kis did not have any significant effect on *shi* mRNA expression (Ghosh et al., 2014). We verified that Kis was not enriched at the *shi* promoter region, and that knockdown of Kis did not have any significant effect on Kis abundance at the *shi* promoter (Figure 2B). In contrast, wild-type control brains showed enrichment of Kis at the three presumptive cis-regulatory sites in the *ecr* locus (*EcR.1*, *EcR.2*, *EcR.3*) (Figure 2B). Upon pan-neuronal knockdown of *Kis-eGFP*, we observed a significant decrease in enrichment at the *fkh* TSS, *EcR.1*, *EcR.2*, and *EcR.3* sites, confirming specificity for Kis binding (Figure 2B). These results suggest that Kis binds to presumptive cis-regulatory sites of the *ecr* locus in *Drosophila* third instar larval brains.

Kismet Does Not Affect Nucleosomal Positioning at the *Ecr* Locus

One mechanism by which chromatin remodeling proteins promote transcriptional activation is by mobilizing nucleosomes and allowing transcriptional machinery access to enhancer sites and promoters of target genes (Clapier et al., 2017). Given Kis's homology to CHD7 and its conserved ATPase domain, we hypothesized that Kis may be remodeling nucleosomes at the *ecr* locus to allow access for the transcriptional machinery. To test this possibility, we immunoprecipitated total histone 3 (H3) protein at the *ecr* locus
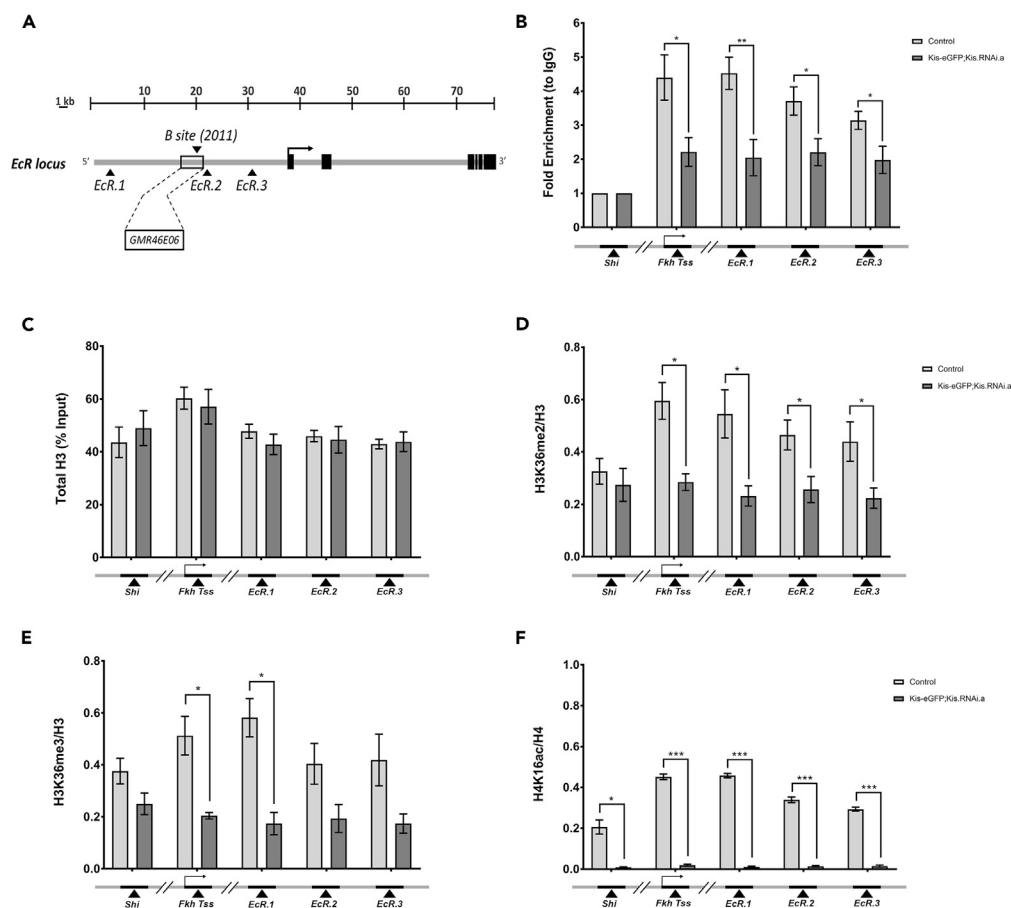
Figure 2. Kis Binds to *Ecr* Locus *In Vivo* Promoting H3K36 Methylation and H4K16 Acetylation

(A) A schematic representation of the *ecr* locus. Black arrowheads upstream of the *ecr-b* TSS (black arrow) indicate location of primers. Black box denotes endogenous location of *GMR46E06-Gal4* enhancer site reporter. B set denotes location of primer set B from Boulanger et al. (Boulanger et al., 2011).

(B) ChIP-qPCR analysis of chromatin isolated from third instar larval brains. Differences in Kis enrichment at the *ecr* enhancer sites (*EcR.1, EcR.2, and EcR.3*), the *fkh* TSS, and the *shi* promoter site between control (*Kis-eGFP*) and Kis knockdown (*elav-Gal4; Kis-eGFP/Kis-eGFP; Kis.RNAi.a/+*) animals displayed (n = 6 biological replicates).

(C) Total H3 as a percentage of the input DNA was determined by qPCR at the previously noted genomic loci (from left to right, n = 5, 8, 8, 8, 8 biological replicates).

(D and E) ChIP-qPCR analysis of (D) H3K36me2 and (E) H3K36me3 abundance relative to total H3 at the above-mentioned genomic loci, respectively (from left to right, n = 2, 4, 4, 4, 4 biological replicates).

(F) ChIP-qPCR analysis of H4K16ac abundance relative to total H4 at the above-mentioned genomic loci (n = 3 biological replicates). Statistical significance is represented by * = $p < 0.05$, ** = $p < 0.01$, and *** = $p < 0.001$. Error bars represent the SEM.

in control and Kis knockdown third instar larval brains. We found no significant difference between these conditions at each of the cis-regulatory loci we analyzed (Figure 2C). To verify this, we performed an MNase protection assay, which utilizes an endo-exonuclease to examine the nucleosomal occupancy at desired loci by quantifying the amount of DNA bound and thus protected by the nucleosomes (Berson et al., 2017). Consistent with our total H3 analysis, we observed no change in the quantity of DNA digested upon Kis knockdown (Figure S5). Taken together, these data suggest that Kis is not affecting the movement of nucleosomes at the *ecr* locus as a mechanism to promote expression of *ecr-b1*.

Kismet Does Not Affect H3K4 or H3K27 Methylation at the *Ecr* Locus

Another way chromatin readers can affect gene expression is by altering the histone modifications present at relevant genomic loci (Clapier et al., 2017), and Kis has been shown to affect histone modifications previously (Srinivasan et al., 2008). We began by analyzing H3K4 methylation states (mono-, di-, and

tri-methylation) at the *ecr* locus in control and Kis knockdown animals, as it is the type of methylation most commonly associated with actively transcribed genes. ChIP-qPCR analysis showed no change in all types of H3K4 methylation levels upon Kis knockdown at these loci (Figures S6A–S6C). We next analyzed H3K27 tri-methylation (H3K27me3), as this modification is often associated with transcriptional repression and has been previously shown to be increased in *kis* mutant polytene salivary glands (Srinivasan et al., 2008). We did not observe any significant change in H3K27me3 upon Kis knockdown at any of the loci examined (Figure S6D). These data suggest that alteration of H3K4 methylation or H3K27 trimethylation is not part of the mechanism by which Kis controls *ecr* gene expression in the *Drosophila* larval CNS.

Kismet Promotes H3K36 Methylation and H4K16 Acetylation

Previous studies demonstrated a global decrease in H3K36me2 and H3K36me3 upon Kis loss in *Drosophila* larval salivary gland polytene chromosomes (Dorighi and Tamkun, 2013). This type of modification is usually associated with actively transcribed genes in *Drosophila* (Dorighi and Tamkun, 2013; Stabell et al., 2007; Wagner and Carpenter, 2012). We therefore sought to determine if the same effect on H3K36 methylation was present in the *Drosophila* larval nervous system upon pan-neural knockdown of Kis protein. We observed that H3K36me2 was significantly decreased at all of the putative *ecr* cis-regulatory sites we analyzed, as well as at the *fkh* positive control, in Kis knockdown brains compared with controls (Figure 2D). Additionally, H3K36me3 was also significantly decreased at *EcR.3* and the *fkh* TSS (Figure 2E). Importantly, this decrease in H3K36 methylation was not global, as there was no significant change with either H3K36 di- or tri-methylation at the *shi* promoter, which is not bound by Kis (Figures 2B, 2D, and 2E). Also, given that H3K36me2 is the substrate for the tri-methylated form, it is likely that the decrease in H3K36me3 is due to the decrease in H3K36me2. Combined, these results suggest Kis affects H3K36me2 and H3K36me3 histone marks at putative cis-regulatory elements upstream of the *ecr* TSS in third instar larval brains.

Previous studies with H3K36me2 have demonstrated a synergistic relationship with other histone modifications, particularly H4K16ac (Bell et al., 2007). H4K16ac directly influences transcription by positively regulating chromatin accessibility to non-histone proteins (Zhang et al., 2017). Additionally, this type of post-translational modification has been shown to negatively impact chromatin condensation by preventing the function of ATP-dependent chromatin-assembly factor, which is involved in the condensation of 30-nm chromatin fibers (Shogren-Knaak et al., 2006; Yang et al., 2006). Since we saw a significant decrease in H3K36me2 at our loci of interest, we wanted to determine if H4K16ac levels were also affected in Kis knockdown animals. ChIP-qPCR revealed that H4K16ac was significantly decreased when Kis was knocked down compared with controls (Figure 2F). This was consistent at all of the loci analyzed, including the *shi* promoter, possibly indicative of a universal decrease in H4K16ac. These results suggest a role for Kismet in maintaining the active histone modifications H3K36me2, H3K36me3, and H4K16ac at cis-regulatory sites as a potential mechanism for activating gene expression.

Kismet Promotes Transcription *In Vivo*

To determine if Kis can specifically control transcriptional output from this genomic area, we utilized a transcriptional reporter that was generated as part of an effort to find putative brain enhancers in *Drosophila* (*GMR46E06-Gal4*, described in Pfeiffer et al., 2008). This reporter drives the expression of transgenic Gal4 protein from a 3,999-kb region endogenously located 16 kb upstream of the *ecr-b* TSS. The 3,999-kb region contains two binding sites of the transcription factor FTZ-F1, which has previously been shown to be required for *ecr* gene expression (Boulanger et al., 2011), and is capable of driving expression of Gal4 in larval, pupal, and adult MBs (Figures 3A and 3B), suggesting this is a *bona fide* enhancer region for *ecr* transcription and underscoring the importance of *GMR46E06* as a CNS enhancer. We hypothesized that, if Kis is required for promoting transcriptional output from this region *in vivo*, then expressing the *UAS:Kis.RNAi* in the *GMR46E06-Gal4* background will decrease Kis protein levels and in turn decrease Gal4 transcriptional output. We therefore measured the levels of *gal4* mRNA and Gal4 protein in control and Kis knockdown brains via RT-qPCR and in MB neurons specifically via immunohistochemistry (Figures 3C–3G). We observed a significant decrease in both *gal4* mRNA and Gal4 protein levels from this reporter in Kis knockdown animals compared with controls, suggesting Kis is required for promoting transcriptional output from this *GMR46E06* region *in vivo* (Figures 3C–3G).

We next wanted to determine if Kis is enriched at this region by performing ChIP-qPCR. We utilized a previously validated site (B site [2011], Figure 2A) within the *GMR46E06* region to test for binding as this site was also bound by the FTZ-F1 transcription factor, which is required for *ecr-b1* gene expression (Boulanger
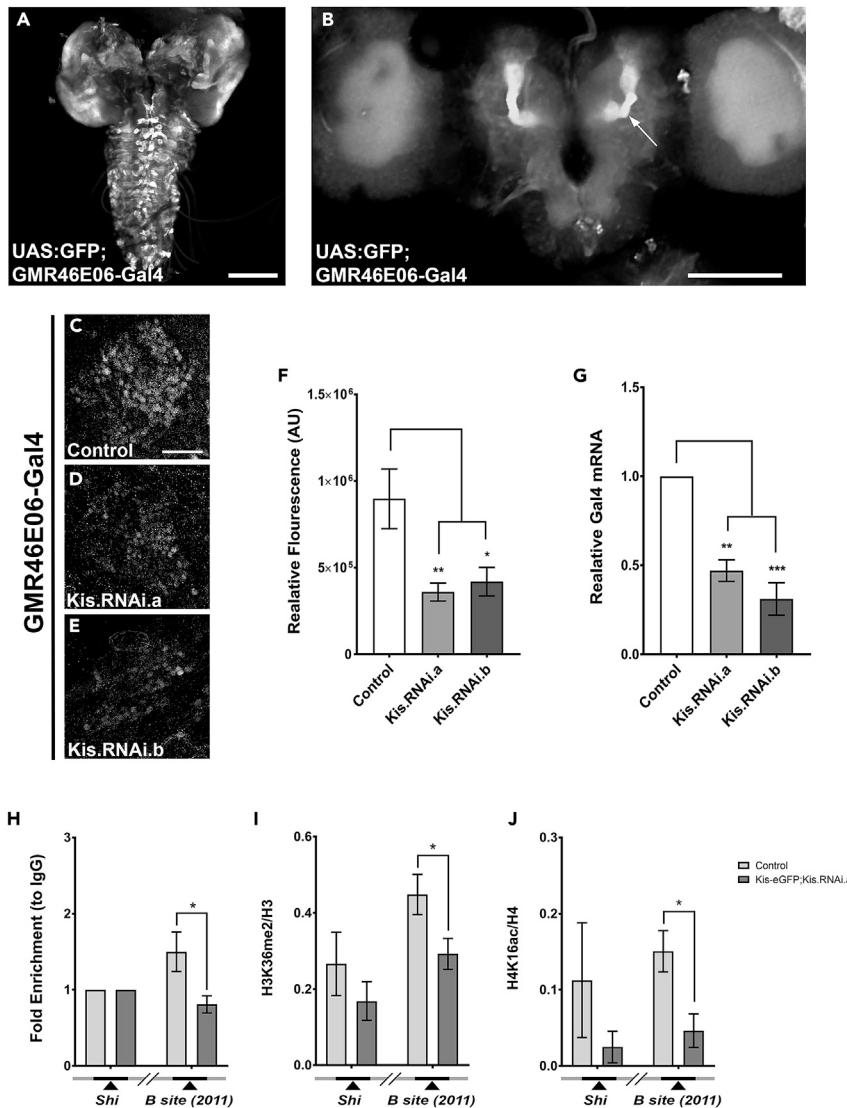
Figure 3. Kis Can Promote Transcription via Putative Enhancer Site 16 kb Upstream of EcR-B TSS

(A and B) Representative images of UAS:GFP; GMR46E06-Gal4 expression in larval and pupal brain, respectively. Arrow in (B) denotes location of MB peduncle area.

(C–E) Representative images of (C) control (w^{1118}) and Kis knockdowns (D) (*UAS:Kis.RNAi.a*) and (E) (*UAS:Kis.RNAi.b*) in larval MB Kenyon cells stained with α-Gal4 expressed using the *GMR46E06-Gal4* enhancer site reporter.

(F) Quantification of fluorescent intensity of α-Gal4 (from left to right, n = 10, 10, 8 MBs).

(G) *gal4* mRNA levels analyzed by RT-qPCR (n = 3, 10 heads/biological replicate).

(H–J) ChIP-qPCR analysis of (H) Kis enrichment, (I) H3K36me2, and (J) H4K16ac at B site 2011 from Boulanger et al., (2011), respectively (from left to right, n = 5, 5, 2, 3, 6, 7 biological replicates).

Scale bars: 4 μm in (A), 100 μm in (B), and 20 μm in (C). Statistical significance is represented by * = p < 0.05, ** = p < 0.01, and *** = p < 0.001. Error bars represent the SEM.

et al., 2011). We found that Kis is enriched at this site and that RNAi-mediated knockdown of Kis-eGFP significantly decreased this enrichment (Figure 3H). We next sought to determine if Kis is also affecting H3K36me2 and H4K16ac modifications at the *GMR46E06* site as it does at the other loci we have tested. We found that loss of Kis significantly decreased both H3K36me2 and H4K16ac (Figures 3I and 3J). Additionally, there was no significant difference in the total histone 3 levels at this site upon Kis knockdown (Figure S7), consistent with our findings at the other loci we analyzed. Taken together, these data suggest that Kis protein can promote transcriptional activation, and potentially increase EcR-B1 expression, by

increasing H3K36me2 and H4K16ac in the *Drosophila* nervous system. Additionally, the Kismet homolog (CHD7) has been suggested to bind to sites distal to TSSs, sites with features suggesting that they are gene enhancer elements. Thus, these data are consistent with at least one other CHD protein binding function (Schnetz et al., 2009).

EcR-B1 Rescues Kis Loss of Function Axon Pruning Defects

EcR-B1 is well documented to be a key player in initiating the axon pruning cascade in MB neurons (Lee et al., 2000; Yu and Schuldiner, 2014). Given that we have shown Kis acts to promote expression of *ecr-b1* in MB neurons from at least one transcriptional enhancer, we sought to determine if we could rescue the pruning defects we observe in *kis* mutants by expressing transgenic EcR-B1. Utilizing the MARCM system, we expressed transgenic EcR-B1 protein within *kis*[LM27] mutant MB clones (Figure 4). We observed that transgenic expression of EcR-B1 significantly reduced the abnormal pruning observed in *kis*[LM27] mutant MB clones (Figures 4B, 4D, and 4E). We also observed a significant reduction in pruning defects when transgenic EcR-B1 was pan-neurally co-expressed with *Kis.RNAi* constructs using the *elav-Gal4,UAS:mCD8-GFP* driver (Figure S8). Interestingly, EcR-B1 overexpression alone, as well as EcR-B1 expression in Kis loss of function backgrounds, produced smaller surface areas in the dorsal and total lobes compared with outcross controls (Figures 4A, 4C, and 4E). This is consistent with Kis functioning upstream of EcR-B1 in the pruning process, as well as with EcR-B1 being the rate-limiting factor for pruning. Therefore, these data suggest that Kis mediates axon pruning in pupal MB neurons by transcriptionally activating *ecr-b1*, thereby controlling EcR-B1 protein levels.

Pruning defects observed during metamorphosis may simply reflect a delay in normal pruning. Therefore, to determine that homozygous MARCM *kis*[LM27] mutant clones indeed have defective developmental pruning, as opposed to having delayed pruning, we sought to determine if the unpruned axons persisted into adulthood. We generated MARCM clones with homozygous *kis*[LM27] MBs (as previously described) and aged the adults for 5 days after eclosion. At the adult stage, the *201y-Gal4* driver is expressed in a subset of alpha and beta neurons in addition to all the gamma neurons (Bornstein et al., 2015). To differentiate, with certainty, between novel pupal-stage generated axons and pre-pupal stage retained axons, we chose to examine an area that should not contain many GFP-positive bundles, i.e., the dorsal lobe. We then immunostained the adult brains with anti-FASII, a transmembrane cell adhesion protein, which is differentially expressed in the separate populations of MB neurons (Bornstein et al., 2015; Stewart and McLean, 2004). FASII expression is lowest in the early born gamma neurons and highest in the late born alpha/beta neurons in adult MBs; therefore, the appearance of GFP-labeled MARCM axons in the dorsal lobe that are weakly or unstained for FASII would constitute aberrant unpruned axons that persisted into adulthood (Bornstein et al., 2015). Compared with control MBs, *kis*[LM27] MARCM clones had significantly more weakly-stained and/or unstained FASII GFP-positive axons outside the dorsal lobe bundle, indicating that pruning is in fact prevented and not delayed in this mutant (Figures 4F–4K and 4R). Given that transgenic expression of EcR-B1 in the *kis*[LM27] MARCM background rescued the pruning defects during the pupal stage, we tested whether transgenic EcR-B1 can also rescue the presence of aberrant axons in adulthood. Expression of EcR-B1 in *kis*[LM27] mutant MARCM clones showed significantly fewer GFP-positive axons outside the dorsal lobe in the adult MB (Figures 4I, 4L–4Q, and 4R). Collectively, these data suggest that the defective pruning observed during metamorphosis in *kis* loss-of-function MB neurons persists into adulthood.

EcR-B1 Rescues Memory Defects

Previous studies from our laboratory showed that reduction of Kis levels in MB neurons produced significant defects in immediate recall memory (Melicharek et al., 2010). Next, we wanted to determine if transgenic expression of EcR-B1 could also rescue the memory defect associated with loss of Kis function. We utilized the conditioned courtship suppression assay, which takes advantage of the innate courting behaviors carried out by male *Drosophila* in response to multimodal signals transduced by females (McBride et al., 2005; Siegel and Hall, 1979; Siwicki et al., 2005). Wild-type males will decrease their rate of courting during a training (learning) period of one hour with an unresponsive female. These males will continue to court at lower rates even with subsequent receptive females for an average of 1–3 h after exposure (McBride et al., 2005; Siegel and Hall, 1979; Siwicki et al., 2005). We utilized *UAS:Kis.RNAi.a* to knock down Kis in MB neurons using the *ok107-Gal4* driver. Importantly, expression of the Gal4 alone or Gal4-mediated expression of transgenic EcR-B1 did not produce any learning (Figure 5A) or memory (Figure 5B) defects. We observed that males with decreased Kis protein displayed intact learning, as evident by the significant decrease in courtship from the initial to final stages of exposure to an unresponsive female
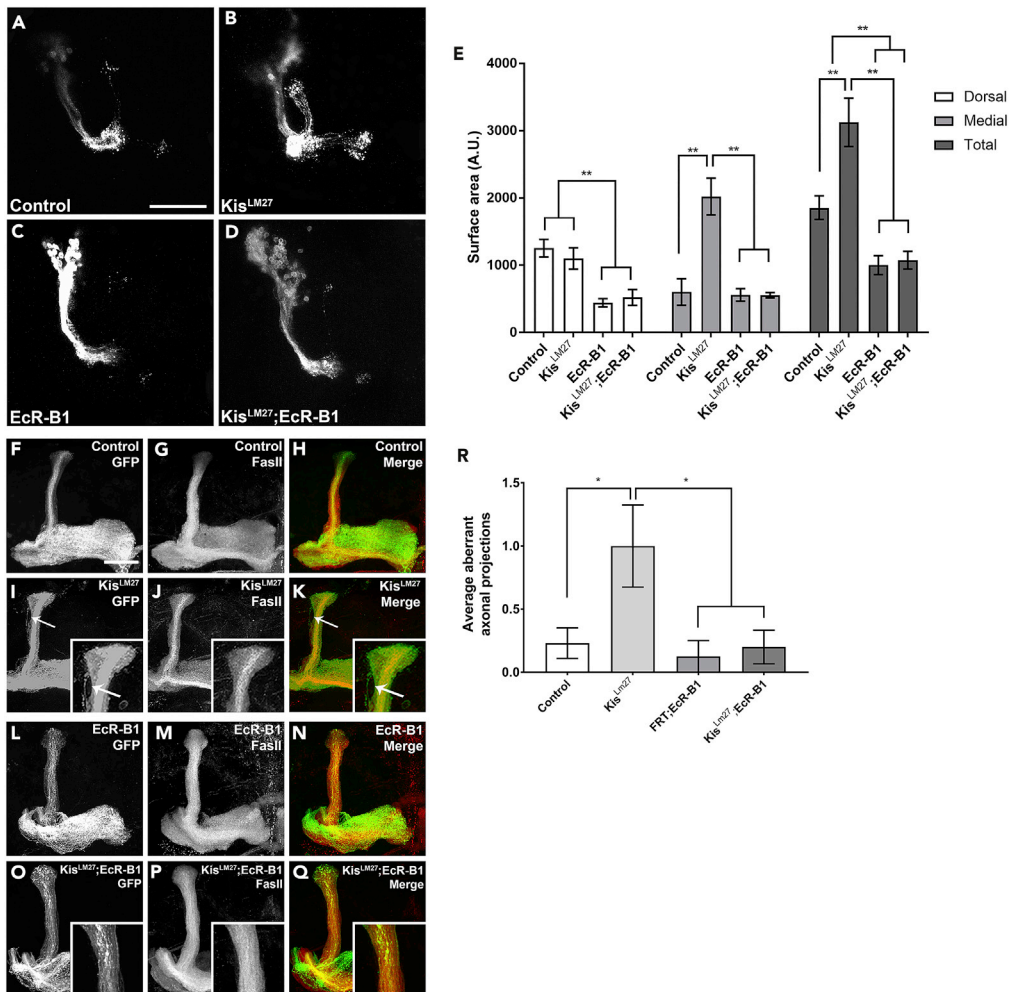
Figure 4. Transgenic EcR-B1 Rescues Defective Axon Pruning Associated with Loss of Kis

(A–D) Representative images of MARCM-generated MB clones expressing membrane-bound GFP using the *201y-Gal4* driver 18–22 h APF. (A) control (*w[1118]; FRT40A*), (B) *kis* null mutant (*Kis[LM27],FRT40A*), (C) EcR-B1 overexpression (*FRT40A; UAS:EcR-B1*), and (D) EcR-B1 rescue (*Kis[LM27],FRT40A; UAS:EcR-B1*).

(E) Quantification of dorsal, medial, and total MB lobe surface areas in MARCM animals (from left to right, n = 12, 11, 10, 12 MBs).

(F–Q) Representative adult MARCM-generated MB clones expressing membrane-bound GFP or stained with α-FasII. (F) control (*w[1118]; FRT40A*) membrane-bound GFP, (G) α-FasII immunostaining, and (H) merge images. (I) *kis* null mutant (*Kis[LM27],FRT40A)* GFP, (J) α-FasII, and (K) merge. (L) EcR-B1 overexpression alone (*FRT40A; UAS:EcR-B1*) GFP, (M) α-FasII immunostaining, and (N) merge. (O) EcR-B1 rescue (*Kis[LM27],FRT40A; UAS:EcR-B1*) GFP, (P) α-FasII immunostaining, and (Q) merge. Arrows indicate aberrant axonal projections in (I) and (K). Insets show magnified area of medial lobes.

(R) Quantification of average aberrant axonal projections in MBs (from left to right, n = 13, 12, 8, 10 MBs).

Scale bars: 10 μm in (A) and 20 μm in (F). Statistical significance is represented by * = p < 0.05, ** = p < 0.01, and *** = p < 0.001. Error bars represent the SEM.

(Figure 5C). Similarly, males with both decreased Kis and transgenic EcR-B1 also had intact learning (Figure 5C). However, males with decreased Kis showed abnormal memory (Figure 5D), as these males had rates of courtship that were not significantly different from those of sham males, which did not receive exposure to an unreceptive female. In contrast, trained males with both decreased Kis and transgenic EcR-B1 showed significantly reduced courtship compared with sham males, indicative of intact immediate recall memory (Figure 5D). Taken together, these data suggest that the memory defects associated with loss of Kis in the MB neurons are due to decreased EcR-B1 levels.
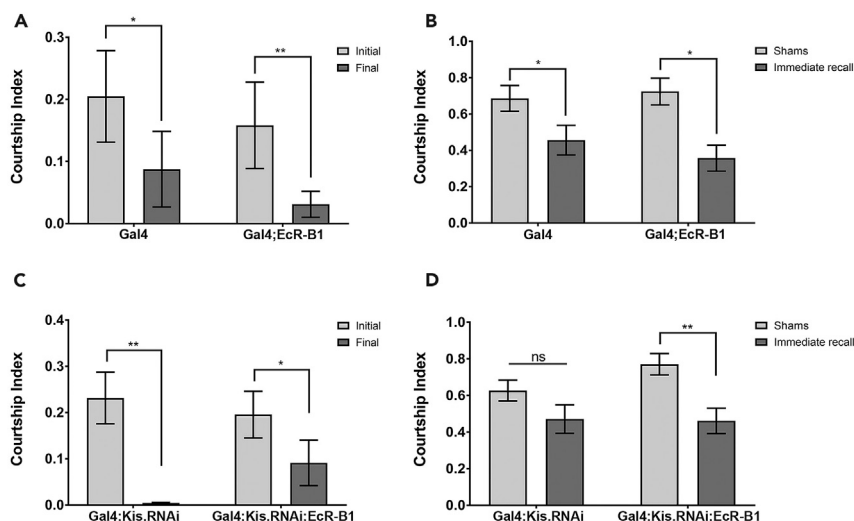
Figure 5. Transgenic EcR-B1 Expression Rescues Memory Defects Rescued in Kis Knockdown MBs

(A and C) Assessment of male courtship index during the initial and final 10 min of the 60-min training period ([A] from left to right, n = 16, 15 males; [C] from left to right, n = 21, 22 males).

(B and D) Immediate recall of trained males was assessed and compared with genetically identical sham trained males ([B] from left to right, n = 14, 13, 13, 15 males; [D] n = 21, 21, 19, 22 males).

Statistical significance is represented by * = p < 0.05 and ** = p < 0.01. Error bars represent the SEM.

SAHA Rescues Morphological and Behavioral Defects Associated with Loss of Kis

Recently, our laboratory showed that pharmacological inhibition of HDACs can rescue multiple defects associated with loss of Kis at the neuromuscular junction (Latcheva et al., 2018). HDAC inhibition (HDACi) did not significantly affect *kis* mRNA levels (Latcheva et al., 2018), so we hypothesized that the rescue may be due to effects on a common set of target genes. To further examine this hypothesis, we tested whether HDACi treatment could rescue the decreased EcR-B1 expression, pruning, and memory defects observed in Kis knockdown animals. We observed that treatment of Kis knockdown with SAHA significantly increased *ecr-b1* mRNA levels compared with DMSO-treated controls (Figure 6S). Importantly, SAHA treatment alone had no significant impact on *ecr-b1* mRNA levels (Figure 6S) or axon pruning in either pupal (Figures 6A, 6B, and 6E) or adult MBs (Figures 6F–6H, 6L–6N, and 6R). However, we did observe that SAHA treatment significantly decreased the number of unpruned axons in both pupal (Figures 6C, 6D, and 6E) and adult brains in *kis*[LM27] mutant MB neurons (Figures 6I–6K, 6O–6Q, and 6R). Finally, SAHA treatment itself did not have an observable impact on learning or memory in controls (Figures 7A and 7B, respectively), or learning in Kis knockdown (Figure 7C). However, SAHA treatment was able to significantly rescue the immediate recall defect in Kis knockdown animals compared with DMSO treatment alone (Figure 7D). In each case, SAHA affected these phenotypes only in *kis* loss-of-function animals, and not in control animals, suggesting a specificity of SAHA interaction with Kis function. SAHA's theraputic effect might be by counteracting the loss of H4K16 acetylation we observed in Kis knockdown animals. Taken together, these results show that HDACi treatment significantly rescues multiple defects associated with Kis loss of function.

DISCUSSION

Axon pruning and elimination are critical steps to establishing and refining neural circuitry. However, relatively little is known about how the precise extrinsic and intrinsic signals come together to initiate the pruning cascade. Here, we begin to unravel the epigenetic mechanisms essential for initiating developmental axon pruning *in vivo*. We show that the chromatin reader Kis activates transcription of *ecr-b1* in the *Drosophila* MBs and promotes methylation of H3K36 and acetylation of H4K16 at cis-regulatory sites of the *ecr-b1* locus. Proper regulation of *ecr-b1* expression by Kis is required for both pruning and immediate recall memory in adults. Finally, we show that the general HDACi, SAHA, can increase *ecr-b1* mRNA levels in animals with decreased Kis and rescue their pruning and memory defects. SAHA may be counteracting the loss of H4K16ac and reestablish a balance of gene expression in Kis knockdown animals. Taken together, our data show that the essential rate-limiting step in developmental axon pruning, EcR-B1 expression, is under the epigenetic control of Kis.
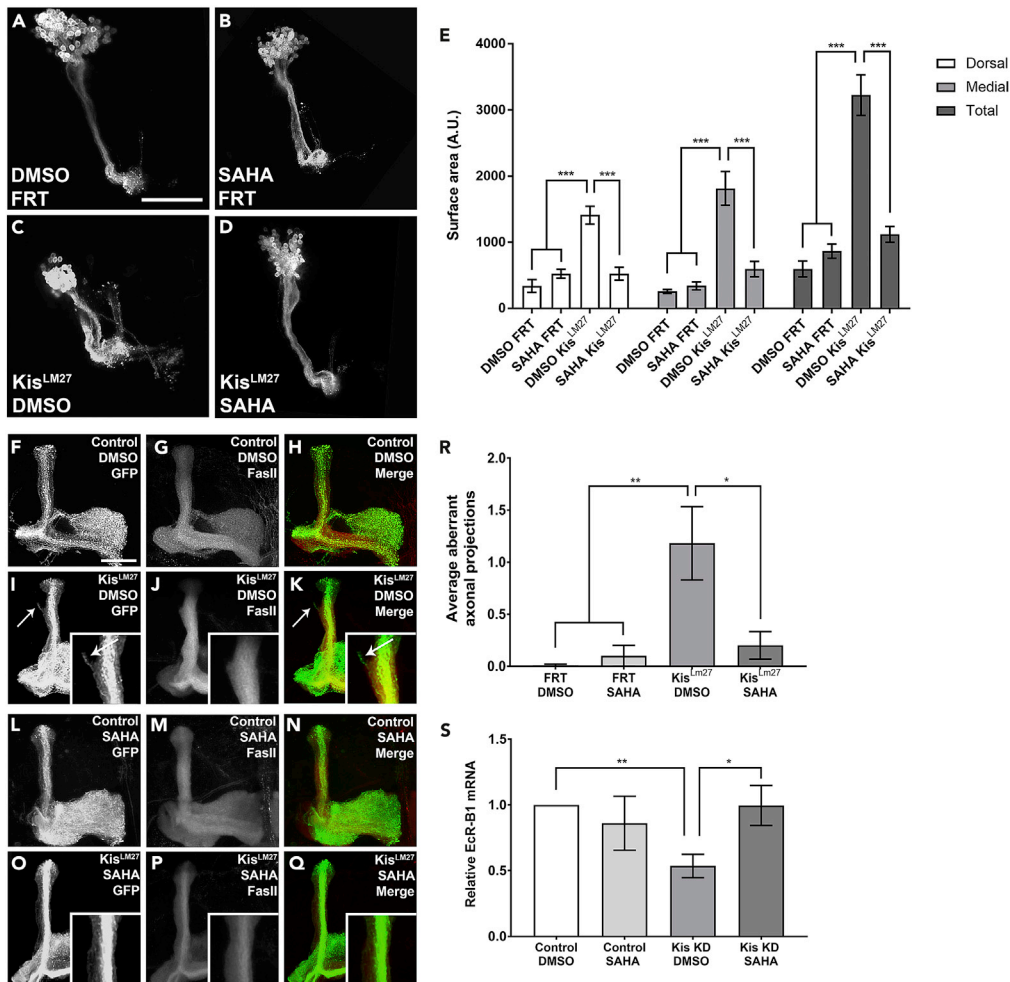
Figure 6. HDAC Inhibition Rescues Defective Axon Pruning and EcR-B1 Expression in Loss of Kis Animals

(A–D) Representative images of DMSO- or SAHA-treated MARCM-generated MB clones expressing GFP using the *201y-Gal4* driver 18–22 h APF. (A) DMSO-treated control (*w*[1118]; *FRT40A*), (B) SAHA-treated control (*w*[1118]; *FRT40A*), (C) DMSO-treated *kis* null mutant (*Kis*[LM27], *FRT40A*), and (D) SAHA-treated *kis* null mutant (*Kis*[LM27],*FRT40A*).

(E) Quantification of dorsal, medial, and total MB lobe surface areas in DMSO- or SAHA-treated MARCM animals (from left to right, n = 11, 11, 11, 10 MBs).

(F–Q) Representative DMSO- or SAHA-treated adult MARCM-generated MB clones expressing membrane-bound GFP or stained with α-FasII. (F) DMSO-treated control (*w*[1118]; *FRT40A*) membrane-bound GFP, (G) α-FasII immunostaining, and (H) merge images. (I) DMSO-treated *kis* null mutant (*Kis*[LM27], *FRT40A*) GFP, (J) α-FasII, and (K) merge. (L) SAHA-treated control (*w*[1118]; *FRT40A*) GFP, (M) α-FasII immunostaining, and (N) merge. (O) SAHA-treated *kis* null mutant (*Kis*[LM27], *FRT40A*) GFP, (P) α-FasII immunostaining, and (Q) merge. Arrows indicate aberrant axonal projections in (I) and (K). Insets show magnified area of medial lobes.

(R) Quantification of average aberrant axonal projections in MBs of flies treated with DMSO or SAHA (from left to right, n = 10, 10, 11, 10 MBs).

(S) *ecr-b1* mRNA levels isolated from DMSO- or SAHA-treated control (*w*[1118]) and pan-neural Kis knockdown (*UAS:Kis.RNAi.a*) pupal heads analyzed by RT-qPCR (number of biological replicates from left to right, n = 4, 3, 4, 4; 10 heads/biological replicate).

Scale bars: 10 μm in (A) and 20 μm in (F). Statistical significance is represented by * = p < 0.05, ** = p < 0.01, and *** = p < 0.001. Error bars represent the SEM.

The expression of *ecr* in the MBs has been subject to studies indicating two distinct pathways of activation (Boulanger et al., 2011; Boulanger and Dura, 2015; Zheng et al., 2003). First, the dTGF-β signaling pathway has been implicated in MB gamma neuron remodeling, as mutations in both the *Drosophila* TGF-β receptor, Baboon, and its downstream effector, dSmad2, produce pruning defects at 18–22 h APF (Zheng et al.,
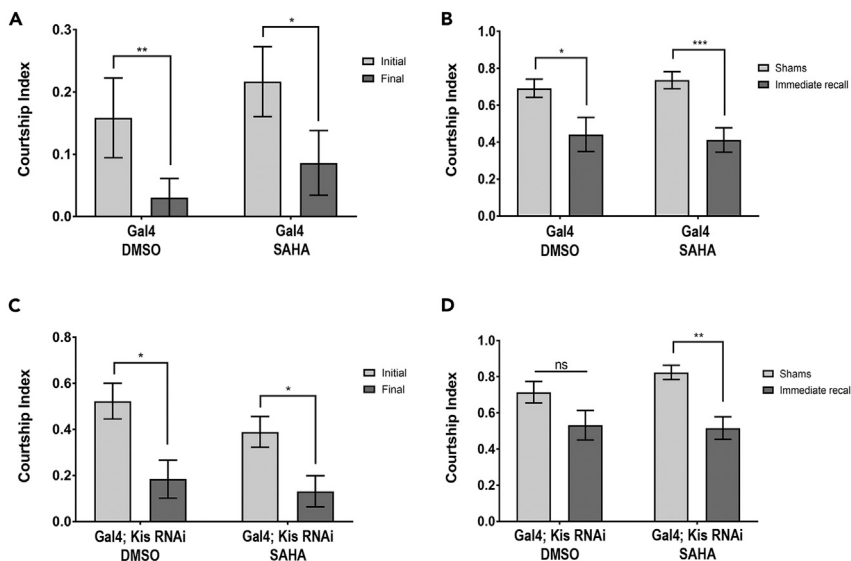
Figure 7. SAHA Treatment Rescues Immediate Recall Defects Rescued in Kis Knockdown Animals

(A and C) Assessment of DMSO- or SAHA-treated male courtship index during the initial and final 10 min of the 60-min training period ([A] from left to right, n = 14, 23 males; [C] from left to right, n = 19, 22 males).

(B and D) Immediate recall of DMSO- or SAHA-treated trained males assessed and compared with sham trained males with identical genetic background and treatment ([B] from left to right, n = 29, 15, 16, 23 males; [D] n = 22, 18, 21, 22 males). Statistical significance is represented by * = p < 0.05 and ** = p < 0.01. Error bars represent the SEM.

2003). Furthermore, transgenic expression of EcR-B1 was able to rescue the pruning defects in the TGF-β pathway mutant backgrounds indicating that EcR-B1 is downstream of TGF-β signaling (Zheng et al., 2003). Similarly, our results demonstrate that transgenic EcR-B1 expression bypassed the need for Kis in a *kis* mutant background and thereby rescued the pruning defects in both pupal and adult MBs. This parallels the previous findings by demonstrating that Kis is upstream of *ecr-b1* transcription. Where Kis fits relative to dTGF-β signaling, however, still remains to be answered.

A second pathway of activating *ecr-b1* transcription in the MBs is via the nuclear receptor Ftz-f1 and its homologue Hr39 (Boulanger et al., 2011; Boulanger and Dura, 2015). Ftz-f1 binds directly to the *ecr* cis-regulatory sites and activates expression of *ecr-b1*, whereas Hr39 acts to block its expression in the MBs (Boulanger et al., 2011). Although this pathway also functions upstream of *ecr-b1* transcription, it is independent of dTGF-β signaling as Ftz-f1 overexpression did not rescue pruning defects in *baboon* mutants (Boulanger et al., 2011). Our data indicate that Kis is also enriched at one cis-regulatory site that Ftz-f1 binds (Figures 2A and 3H), but whether they act in coordination or independently of each other remains to be determined. It may be that both Kis and Ftz-f1 act independently and help create redundancy in case of the failure of one pathway. Given that reduction of neither Kis nor Ftz-f1 completely eliminated EcR-B1 levels may support this redundancy hypothesis; however, more work is necessary to explore their relationship (Boulanger et al., 2011).

Few studies have hinted at an epigenetic mechanism of *ecr* transcriptional activation. The *Drosophila* Set2 K36 histone methyl transferase (HMT) was shown to genetically interact with the EcR signaling pathway and positively regulate expression of EcR target genes (Stabell et al., 2007). However, as dSet2 is required for general transcriptional elongation, this may be a global effect of dSet2 function. Nonetheless, this implicates H3K36 methylation as an important factor in *ecr* expression. Although Kis does not appear to affect expression of *Drosophila set2*, and the other H3K36 HMT genes *ash1* or *dmes-4* (data not shown), it might be acting to recruit the HMTs to relevant target genes to transduce effects on transcriptional regulation. To this effect, Kis was previously shown to increase the global association of Ash1 on polytene chromosomes (Dorighi and Tamkun, 2013). Although other studies with Kis have implied a role for the chromatin reader in transcriptional elongation (Srinivasan et al., 2005, 2008), we demonstrate a selectivity for Kis binding and Kis-mediated elevation of H3K36 methylation as no significant changes were observed at the *shi* promoter in Kis knockdown animals. Further work

needs to be done to tease apart the relationship between Kis, H3K36 methylation, and any other HMTs responsible for this modification in the context of *ecr* regulation.

In the field of epigenetics, much work has been done to understand the cross talk between different histone modifications and their cumulative outcome on transcription. For example, H3K36me2 by the HMT dMes-4 was reported to specifically increase H4K16ac, a modification most well known for its role in decondensation of chromatin structure and maintenance of active gene expression (Bell et al., 2007; Shogren-Knaak et al., 2006; Zhang et al., 2017). We provide evidence for this type of epigenetic cross talk by demonstrating a targeted loss of H3K36 methylation as well as a loss of H4K16 acetylation in a Kis knockdown background. It is therefore plausible that Kis might be affecting transcriptional output by promoting H4K16ac via H3K36me2 cross talk. This may explain why HDAC inhibition with SAHA, seemingly unrelated to histone methylation, is able to restore *ecr-b1* mRNA levels and rescue pruning and memory defects associated with loss of Kis. Consistent with this, SAHA treatment has been previously shown to increase H4K16ac and ultimately increase transcriptional output in cancer cells (Barbetti et al., 2013). Additionally, it may be the case that general HDAC inhibition by SAHA may be universally increasing transcription in a non-specific manner. However, we show here that SAHA treatment alone does not significantly affect either *ecr-b1* mRNA levels or axon pruning. Therefore, the phenotypic effects we observe with SAHA treatment are specific to animals where Kis function is decreased. Additional work is essential to building a complete understanding of the integration of extrinsic and intrinsic cues that control transcriptional regulation.

One interesting observation from our work is that Kis appears to affect pruning of the medial lobes of the MB, while largely leaving the dorsal lobes unaffected. This was the case for both our MARCM analysis as well as our RNAi analysis. It is well established that Ecr-B1 is required for axon pruning of both the dorsal and medial lobes (Lee et al., 2000). Indeed, our data further confirm this, as Ecr-B1 expression does show an effect on the pruning of both the dorsal and medial lobes (Figure 4). Thus, these data suggest that Kis must not be regulating axon pruning solely by promoting the transcription of *ecr-b1* and may also be modulating some other factor that can discriminate between dorsal and medial lobes. Recent work has shown that the neuronal architecture of the MB is quite extensive and forms 15 distinct compartments that tile the MB lobes (Aso et al., 2014a, 2014b). Thus, Kis may only be affecting *ecr-b1* expression and pruning in a subset of the neurons that innervate the medial lobes, or, alternately, may be affecting additional factors besides Ecr-B1 that can discriminate pruning between these two lobes. Determining what these factors may be will require additional work.

In summary, our work has helped to shed light on the epigenetic factors that are involved in the regulated developmental pruning required in Drosophila MB neurons. Determining how axons are properly pruned is fundamental to unraveling the mechanisms that underlie the refinement of neural circuits.

Limitations of the Study

One limitation of the current study is the method we use to overexpress the Kismet protein, in that the overexpressed RNA can be targeted by our RNAi strategy. Future studies should consider utilizing an overexpression transgene that cannot be targeted by RNAi. A second limitation to the current study is that fact that, although we have identified a protein that differentially affects pruning in the medial vs. the dorsal lobes of the MB, we cannot fully explain how Kismet was able to accomplish this. Future studies should be cognizant that proteins may regulate the pruning of MB lobes differently.

METHODS

All methods can be found in the accompanying Transparent Methods supplemental file.

SUPPLEMENTAL INFORMATION

Supplemental Information can be found online at https://doi.org/10.1016/j.isci.2019.05.021.

AUTHOR CONTRIBUTIONS

Conceptualization, N.K.L., J.M.V., D.R.M.; Methodology, N.K.L., J.M.V., D.R.M.; Validation, N.K.L., J.M.V.; Formal Analysis, N.K.L., J.M.V., D.R.M.; Investigation, N.K.L., J.M.V.; Writing – Original Draft, N.K.L., J.M.V., D.R.M.; Writing – Review & Editing, N.K.L., J.M.V., D.R.M.; Supervision, D.R.M.; Project Administration, D.R.M.; Funding Acquisition, D.R.M.

DECLARATIONS OF INTERESTS

The authors declare no competing interests.

REFERENCES

Ashburner, M. (1974). Sequential gene activation by ecdysone in polytene chromosomes of *Drosophila melanogaster*. II. The effects of inhibitors of protein synthesis. Dev. Biol. *39*, 141–157.

Ashburner, M., Chihara, C., Meltzer, P., and Richards, G. (1974). Temporal control of puffing activity in polytene chromosomes. Cold Spring Harb. Symp. Quant. Biol. *38*, 655–662.

Aso, Y., Hattori, D., Yu, Y., Johnston, R.M., Iyer, N.A., Ngo, T.T., Dionne, H., Abbott, L.F., Axel, R., Tanimoto, H., et al. (2014a). The neuronal architecture of the mushroom body provides a logic for associative learning. Elife *3*, e04577.

Aso, Y., Sitaraman, D., Ichinose, T., Kaun, K.R., Vogt, K., Belliart-Guerin, G., Placais, P.Y., Robie, A.A., Yamagata, N., Schnaitmann, C., et al. (2014b). Mushroom body output neurons encode valence and guide memory-based action selection in Drosophila. Elife *3*, e04580.

Awasaki, T., Huang, Y., O'Connor, M.B., and Lee, T. (2011). Glia instruct developmental neuronal remodeling through TGF-beta signaling. Nat. Neurosci. *14*, 821–823.

Barbetti, V., Gozzini, A., Cheloni, G., Marzi, I., Fabiani, E., Santini, V., Dello Sbarba, P., and Rovida, E. (2013). Time- and residue-specific differences in histone acetylation induced by VPA and SAHA in AML1/ETO-positive leukemia cells. Epigenetics *8*, 210–219.

Bell, O., Wirbelauer, C., Hild, M., Scharf, A.N., Schwaiger, M., MacAlpine, D.M., Zilbermann, F., van Leeuwen, F., Bell, S.P., Imhof, A., et al. (2007). Localized H3K36 methylation states define histone H4K16 acetylation during transcriptional elongation in Drosophila. EMBO J. *26*, 4974–4984.

Berson, A., Sartoris, A., Nativio, R., Van Deerlin, V., Toledo, J.B., Porta, S., Liu, S., Chung, C.Y.,

Garcia, B.A., Lee, V.M., et al. (2017). TDP-43 promotes neurodegeneration by impairing chromatin remodeling. Curr. Biol. *27*, 3579–3590.e6.

Bornstein, B., Zahavi, E.E., Gelley, S., Zoosman, M., Yaniv, S.P., Fuchs, O., Porat, Z., Perlson, E., and Schuldiner, O. (2015). Developmental axon pruning requires destabilization of cell adhesion by JNK signaling. Neuron *88*, 926–940.

Boulanger, A., Clouet-Redt, C., Farge, M., Flandre, A., Guignard, T., Fernando, C., Juge, F., and Dura, J.M. (2011). ftz-f1 and Hr39 opposing roles on EcR expression during Drosophila mushroom body neuron remodeling. Nat. Neurosci. *14*, 37–44.

Boulanger, A., and Dura, J.M. (2015). Nuclear receptors and Drosophila neuronal remodeling. Biochim. Biophys. Acta *1849*, 187–195.

Buszczak, M., Paterno, S., Lighthouse, D., Bachman, J., Planck, J., Owen, S., Skora, A.D., Nystul, T.G., Ohlstein, B., Allen, A., et al. (2007). The carnegie protein trap library: a versatile tool for Drosophila developmental studies. Genetics *175*, 1505–1531.

Clapier, C.R., Iwasa, J., Cairns, B.R., and Peterson, C.L. (2017). Mechanisms of action and regulation of ATP-dependent chromatin-remodelling complexes. Nat. Rev. Mol. Cell Biol. *18*, 407–422.

Connolly, J.B., Roberts, I.J., Armstrong, J.D., Kaiser, K., Forte, M., Tully, T., and O'Kane, C.J. (1996). Associative learning disrupted by impaired Gs signaling in Drosophila mushroom bodies. Science *274*, 2104–2107.

Dorighi, K.M., and Tamkun, J.W. (2013). The trithorax group proteins Kismet and ASH1 promote H3K36 dimethylation to counteract Polycomb group repression in Drosophila. Development *140*, 4182–4192.

Ferveur, J.F., Stortkuhl, K.F., Stocker, R.F., and Greenspan, R.J. (1995). Genetic feminization of brain structures and changed sexual orientation in male Drosophila. Science *267*, 902–905.

Ghosh, R., Vegesna, S., Safi, R., Bao, H., Zhang, B., Marenda, D.R., and Liebl, F.L. (2014). Kismet positively regulates glutamate receptor localization and synaptic transmission at the Drosophila neuromuscular junction. PLoS One *9*, e113494.

Handler, A.M. (1982). Ecdysteroid titers during pupal and adult development in *Drosophila melanogaster*. Dev. Biol. *93*, 73–82.

Heisenberg, M., Borst, A., Wagner, S., and Byers, D. (1985). Drosophila mushroom body mutants are deficient in olfactory learning. J. Neurogenet. *2*, 1–30.

Ishimoto, H., Sakai, T., and Kitamoto, T. (2009). Ecdysone signaling regulates the formation of long-term courtship memory in adult *Drosophila melanogaster*. Proc. Natl. Acad. Sci. U S A *106*, 6381–6386.

Ito, K., Awano, W., Suzuki, K., Hiromi, Y., and Yamamoto, D. (1997). The Drosophila mushroom body is a quadruple structure of clonal units each of which contains a virtually identical set of neurones and glial cells. Development *124*, 761–771.

Lai, Y.W., Chu, S.Y., Wei, J.Y., Cheng, C.Y., Li, J.C., Chen, P.L., Chen, C.H., and Yu, H.H. (2016). Drosophila microRNA-34 impairs axon pruning of mushroom body gamma neurons by downregulating the expression of ecdysone receptor. Sci. Rep. *6*, 39141.

Latcheva, N.K., Viveiros, J.M., Waddell, E.A., Nguyen, P.T.T., Liebl, F.L.W., and Marenda, D.R. (2018). Epigenetic crosstalk: pharmacological inhibition of HDACs can rescue defective synaptic morphology and neurotransmission

phenotypes associated with loss of the chromatin reader Kismet. Mol. Cell Neurosci. *87*, 77–85.

Layman, W.S., Hurd, E.A., and Martin, D.M. (2010). Chromodomain proteins in development: lessons from CHARGE syndrome. Clin. Genet. *78*, 11–20.

Lee, T., Lee, A., and Luo, L. (1999). Development of the Drosophila mushroom bodies: sequential generation of three distinct types of neurons from a neuroblast. Development *126*, 4065–4076.

Lee, T., and Luo, L. (1999). Mosaic analysis with a repressible cell marker for studies of gene function in neuronal morphogenesis. Neuron *22*, 451–461.

Lee, T., Marticke, S., Sung, C., Robinow, S., and Luo, L. (2000). Cell-autonomous requirement of the USP/EcR-B ecdysone receptor for mushroom body neuronal remodeling in Drosophila. Neuron *28*, 807–818.

Levine, R.B., Morton, D.B., and Restifo, L.L. (1995). Remodeling of the insect nervous system. Curr. Opin. Neurobiol. *5*, 28–35.

Low, L.K., and Cheng, H.J. (2006). Axon pruning: an essential step underlying the developmental plasticity of neuronal connections. Philos. Trans. R. Soc. Lond. B Biol. Sci. *361*, 1531–1544.

McBride, S.M., Choi, C.H., Wang, Y., Liebelt, D., Braunstein, E., Ferreiro, D., Sehgal, A., Siwicki, K.K., Dockendorff, T.C., Nguyen, H.T., et al. (2005). Pharmacological rescue of synaptic plasticity, courtship behavior, and mushroom body defects in a Drosophila model of fragile X syndrome. Neuron *45*, 753–764.

McBride, S.M., Giuliani, G., Choi, C., Krause, P., Correale, D., Watson, K., Baker, G., and Siwicki, K.K. (1999). Mushroom body ablation impairs short-term memory and long-term memory of courtship conditioning in *Drosophila melanogaster*. Neuron *24*, 967–977.

Melicharek, D., Shah, A., DiStefano, G., Gangemi, A.J., Orapallo, A., Vrailas-Mortimer, A.D., and Marenda, D.R. (2008). Identification of novel regulators of atonal expression in the developing Drosophila retina. Genetics *180*, 2095–2110.

Melicharek, D.J., Ramirez, L.C., Singh, S., Thompson, R., and Marenda, D.R. (2010). Kismet/CHD7 regulates axon morphology, memory and locomotion in a Drosophila model of CHARGE syndrome. Hum. Mol. Genet. *19*, 4253–4264.

Pfeiffer, B.D., Jenett, A., Hammonds, A.S., Ngo, T.T.B., Misra, S., Murphy, C., Scully, A., Carlson, J.W., Wan, K.H., Laverty, T.R., et al. (2008). Tools for neuroanatomy and neurogenetics in Drosophila. Proc. Natl. Acad. Sci. U S A *105*, 9715–9720.

Redt-Clouet, C., Trannoy, S., Boulanger, A., Tokmatcheva, E., Savvateeva-Popova, E., Parmentier, M.L., Preat, T., and Dura, J.M. (2012).

Mushroom body neuronal remodelling is necessary for short-term but not for long-term courtship memory in Drosophila. Eur. J. Neurosci. *35*, 1684–1691.

Schnetz, M.P., Bartels, C.F., Shastri, K., Balasubramanian, D., Zentner, G.E., Balaji, R., Zhang, X., Song, L., Wang, Z., Laframboise, T., et al. (2009). Genomic distribution of CHD7 on chromatin tracks H3K4 methylation patterns. Genome Res. *19*, 590–601.

Schuldiner, O., Berdnik, D., Levy, J.M., Wu, J.S., Luginbuhl, D., Gontang, A.C., and Luo, L. (2008). piggyBac-based mosaic screen identifies a postmitotic function for cohesin in regulating developmental axon pruning. Dev. Cell *14*, 227–238.

Shogren-Knaak, M., Ishii, H., Sun, J.M., Pazin, M.J., Davie, J.R., and Peterson, C.L. (2006). Histone H4-K16 acetylation controls chromatin structure and protein interactions. Science *311*, 844–847.

Siegel, R.W., and Hall, J.C. (1979). Conditioned responses in courtship behavior of normal and mutant Drosophila. Proc. Natl. Acad. Sci. U S A *76*, 3430–3434.

Siwicki, K.K., Riccio, P., Ladewski, L., Marcillac, F., Dartevelle, L., Cross, S.A., and Ferveur, J.F. (2005). The role of cuticular pheromones in courtship conditioning of Drosophila males. Learn. Mem. *12*, 636–645.

Spindler, S.R., and Hartenstein, V. (2010). The Drosophila neural lineages: a model system to study brain development and circuitry. Dev. Genes Evol. *220*, 1–10.

Srinivasan, S., Armstrong, J.A., Deuring, R., Dahlsveen, I.K., McNeill, H., and Tamkun, J.W. (2005). The Drosophila trithorax group protein Kismet facilitates an early step in transcriptional elongation by RNA Polymerase II. Development *132*, 1623–1635.

Srinivasan, S., Dorighi, K.M., and Tamkun, J.W. (2008). Drosophila Kismet regulates histone H3 lysine 27 methylation and early elongation by RNA polymerase II. PLoS Genet. *4*, e1000217.

Stabell, M., Larsson, J., Aalen, R.B., and Lambertsson, A. (2007). Drosophila dSet2 functions in H3-K36 methylation and is required for development. Biochem. Biophys. Res. Commun. *359*, 784–789.

Stewart, B.A., and McLean, J.R. (2004). Population density regulates Drosophila synaptic morphology in a Fasciclin-II-dependent manner. J. Neurobiol. *61*, 392–399.

Talbot, W.S., Swyryd, E.A., and Hogness, D.S. (1993). Drosophila tissues with different metamorphic responses to ecdysone express different ecdysone receptor isoforms. Cell *73*, 1323–1337.

Tau, G.Z., and Peterson, B.S. (2010). Normal development of brain circuits. Neuropsychopharmacology *35*, 147–168.

Technau, G., and Heisenberg, M. (1982). Neural reorganization during metamorphosis of the corpora pedunculata in *Drosophila melanogaster*. Nature *295*, 405–407.

Thummel, C.S. (2002). Ecdysone-regulated puff genes 2000. Insect Biochem. Mol. Biol. *32*, 113–120.

Truman, J.W. (1990). Metamorphosis of the central nervous system of Drosophila. J. Neurobiol. *21*, 1072–1084.

Truman, J.W., Talbot, W.S., Fahrbach, S.E., and Hogness, D.S. (1994). Ecdysone receptor expression in the CNS correlates with stage-specific responses to ecdysteroids during Drosophila and Manduca development. Development *120*, 219–234.

Vissers, L.E., van Ravenswaaij, C.M., Admiraal, R., Hurst, J.A., de Vries, B.B., Janssen, I.M., van der Vliet, W.A., Huys, E.H., de Jong, P.J., Hamel, B.C., et al. (2004). Mutations in a new member of the chromodomain gene family cause CHARGE syndrome. Nat. Genet. *36*, 955–957.

Wagner, E.J., and Carpenter, P.B. (2012). Understanding the language of Lys36 methylation at histone H3. Nat. Rev. Mol. Cell Biol. *13*, 115–126.

Yamanaka, N., Rewitz, K.F., and O'Connor, M.B. (2013). Ecdysone control of developmental transitions: lessons from Drosophila research. Annu. Rev. Entomol. *58*, 497–516.

Yang, J.G., Madrid, T.S., Sevastopoulos, E., and Narlikar, G.J. (2006). The chromatin-remodeling enzyme ACF is an ATP-dependent DNA length sensor that regulates nucleosome spacing. Nat. Struct. Mol. Biol. *13*, 1078–1083.

Yang, M.Y., Armstrong, J.D., Vilinsky, I., Strausfeld, N.J., and Kaiser, K. (1995). Subdivision of the Drosophila mushroom bodies by enhancer-trap expression patterns. Neuron *15*, 45–54.

Yu, F., and Schuldiner, O. (2014). Axon and dendrite pruning in Drosophila. Curr. Opin. Neurobiol. *27*, 192–198.

Zhang, R., Erler, J., and Langowski, J. (2017). Histone acetylation regulates chromatin accessibility: role of H4K16 in inter-nucleosome interaction. Biophys. J. *112*, 450–459.

Zheng, X., Wang, J., Haerry, T.E., Wu, A.Y., Martin, J., O'Connor, M.B., Lee, C.H., and Lee, T. (2003). TGF-beta signaling activates steroid hormone receptor expression during neuronal remodeling in the Drosophila brain. Cell *112*, 303–315.

Supplemental Information

The *Drosophila* Chromodomain Protein Kismet

Activates Steroid Hormone Receptor Transcription

to Govern Axon Pruning and Memory *In Vivo*

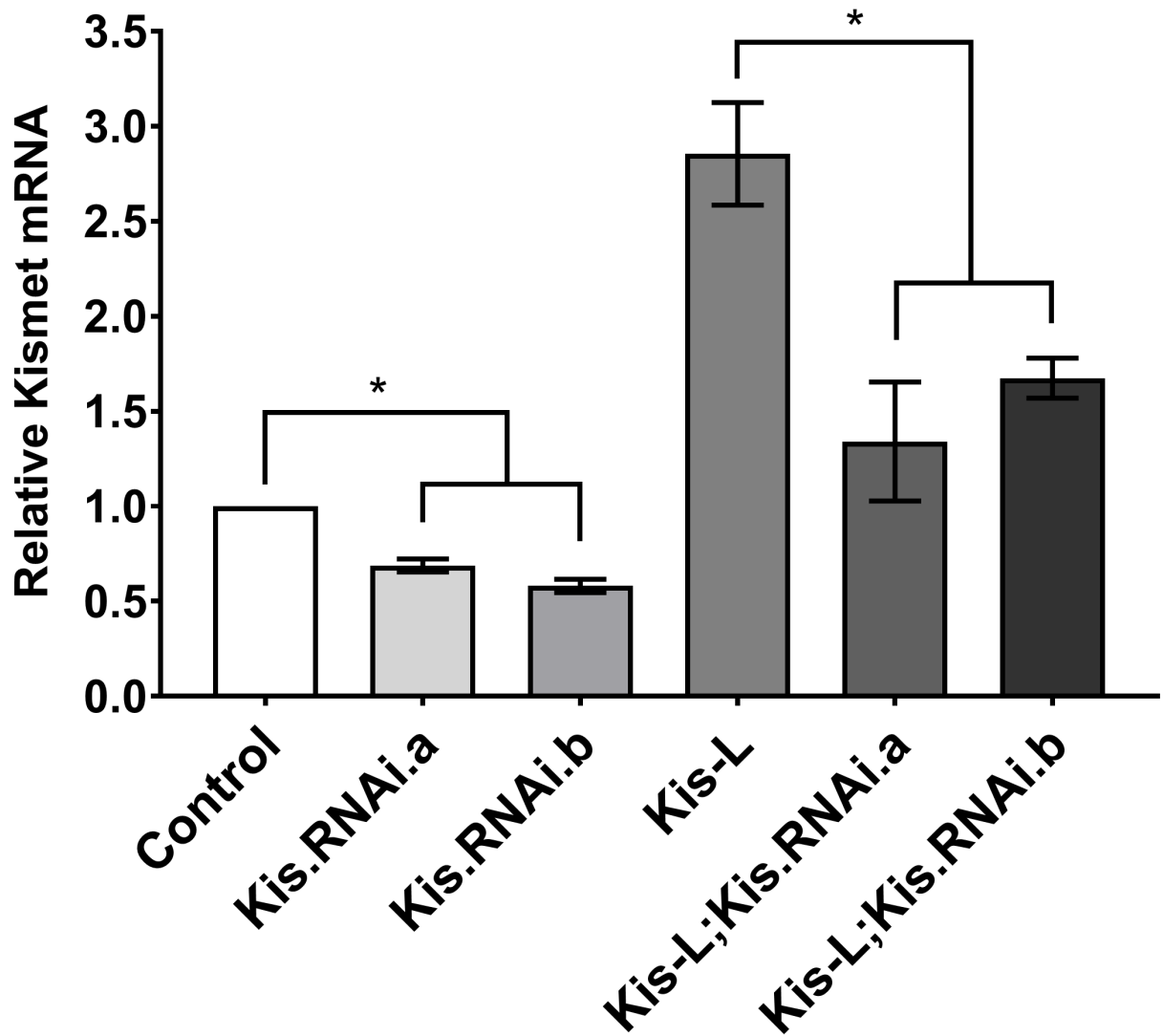Nina K. Latcheva, Jennifer M. Viveiros, and Daniel R. Marenda

Figure S1. Exogenous Kis rescues Kis transcript levels in Kis RNAi animals, related to Figure 1. Quantification of *kis* mRNA levels of control (*w^1118^*), Kis knockdown (*UAS:kis RNAi.a* and *UAS:kis RNAi.b*), Kis overexpression (*UAS:kis-L*), and Kis rescue (*UAS:kis-L; UAS:kis RNAi.a* and *UAS:kis-L,UAS:kis RNAi.b*) pupal brains analyzed by RT-qPCR (n = 5, 3, 3, 3, 3, 5; 10 brains/ biological replicate). Error bars represent the SEM.
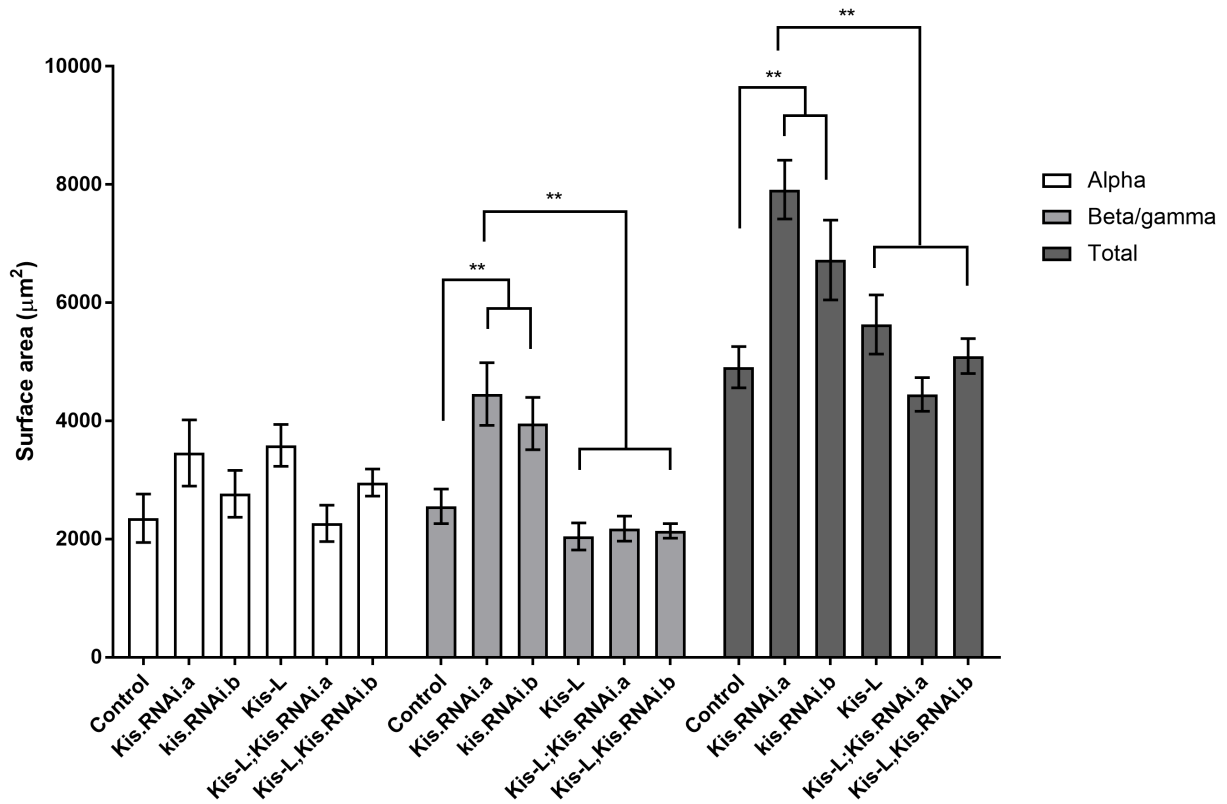
Figure S2. Kis is required for axon pruning in Kis knockdown pupae, related to Figure 1. Quantification of dorsal, medial, and total MB lobe surface areas in control (w^{1118}), Kis knockdown (*UAS:Kis.RNAi.a* and *UAS:Kis.RNAi.b*), Kis overexpression (*UAS:Kis-L*), and Kis rescue (*UAS:Kis-L; UAS:Kis.RNAi.a* and *UAS:Kis-L,UAS:Kis.RNAi.b*) using the *elav-Gal-4,UAS:mCD8-GFP* driver 18-22 hrs APF (from left to right, n = 9, 9, 8, 8, 9, 10 MBs). Statistical significance is represented by * = $p < 0.05$ and ** = $p < 0.01$. Error bars represent the SEM.
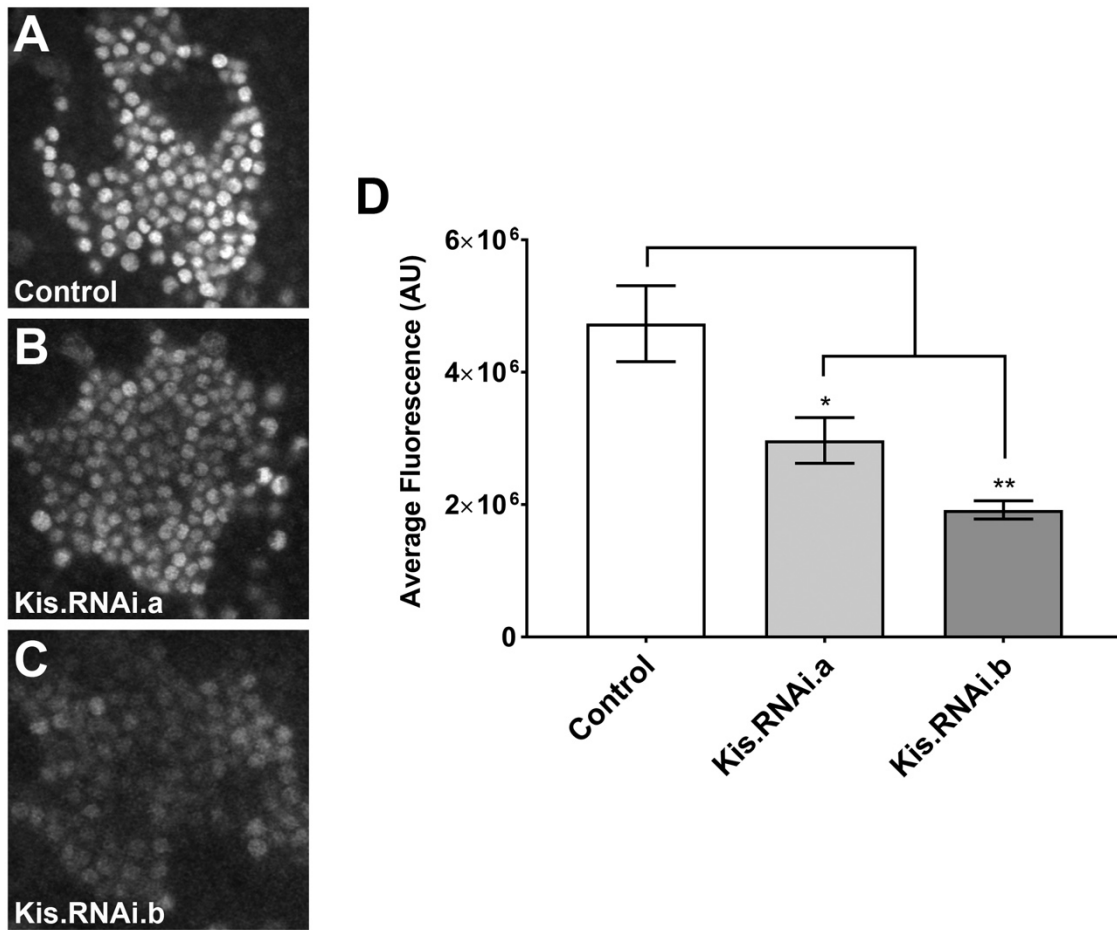
Figure S3. Kis knockdown decreases EcR-B1 expression in late 3rd instar larva, related to Figure 1. (A-C) Representative images of EcR-B1 in control (w^{1118}) and Kis knockdown (*UAS:kis RNAi.a* and *UAS:kis RNAi.b*) late 3rd instar larval Kenyon cells using the *elav-Gal4* driver. (D) Quantification of EcR-B1 within larval Kenyon cells via average fluorescence (n = 5, 6, 4 MBs). Error bars represent the SEM.
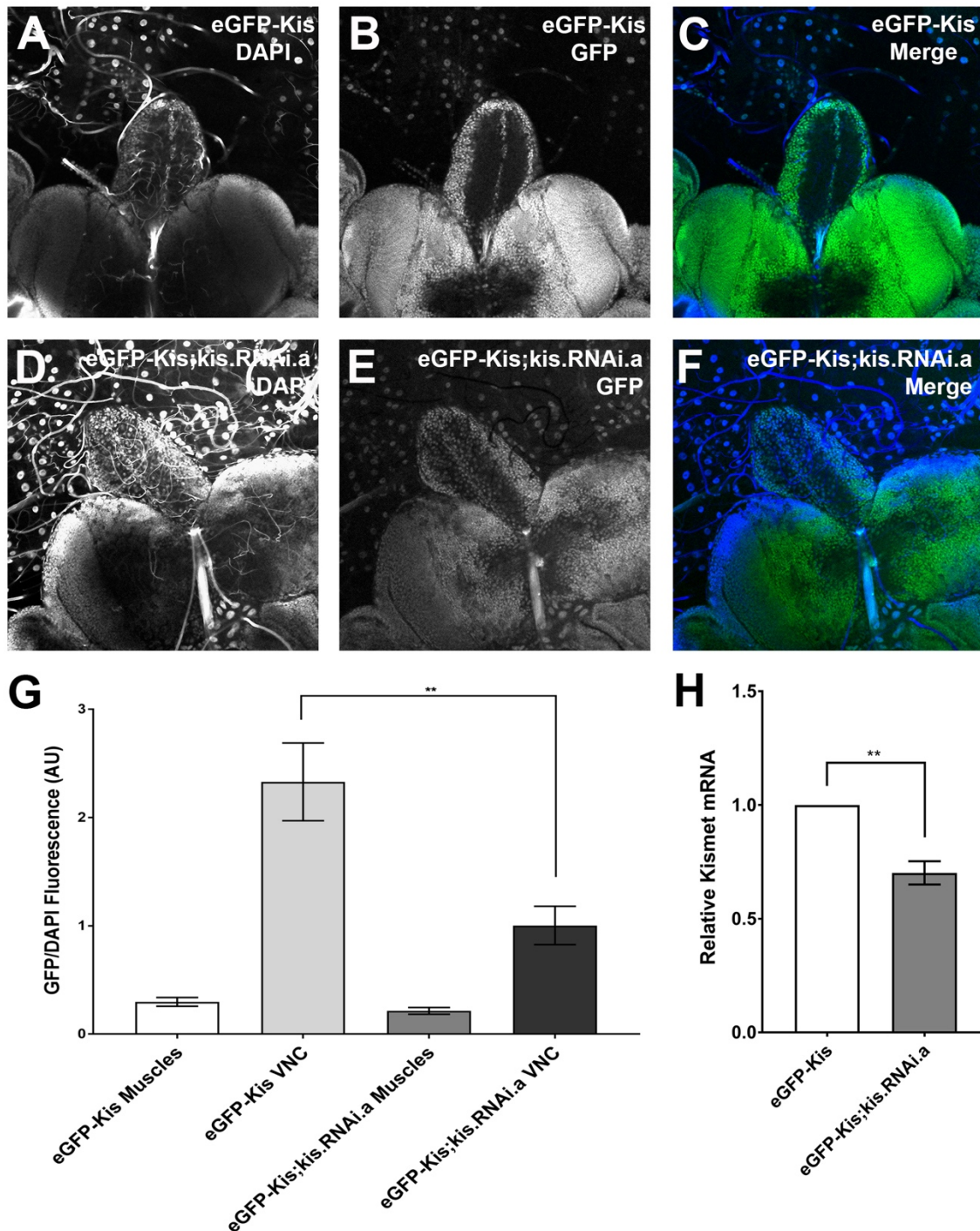
Figure S4. Kis-eGFP is knocked down by Kis.RNAi.a, related to Figure 2. (A-F) Representative images of *Kis-eGFP* (control) and *elav-Gal4; Kis-eGFP/Kis-eGFP; kis RNAi.a/+* (Kis knockdown) 3rd instar larval brains stained with DAPI. (G) Quantification of GFP fluorescence intensity compared to that of DAPI (n = 6). (H) *kis* mRNA levels of control and Kis knockdown 3rd instar larval brains analyzed by RT-qPCR (n = 4, 50 brains/ biological replicate). Statistical significance is represented by ** = $p < 0.01$. Error bars represent the SEM.
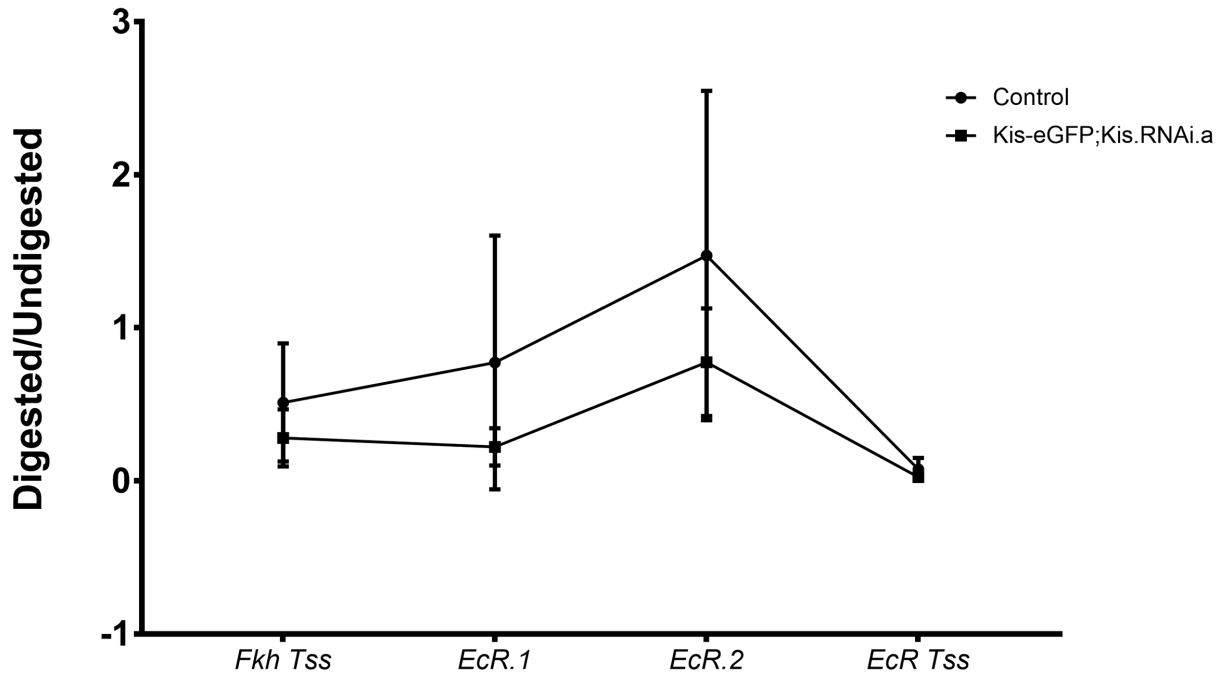
Figure S5. Kis does not alter DNA protection at *EcR* loci, related to Figure 2. Quantification of MNase protection assay using *Kis-eGFP* (control) and *elav-Gal4; Kis-eGFP/Kis-eGFP; Kis.RNAi.a/+* (Kis knockdown) 3rd instar larval brains by qPCR at the *ecr* enhancer sites and the *fkh* TSS (n = 6 biological replicates). Error bars represent the SEM.
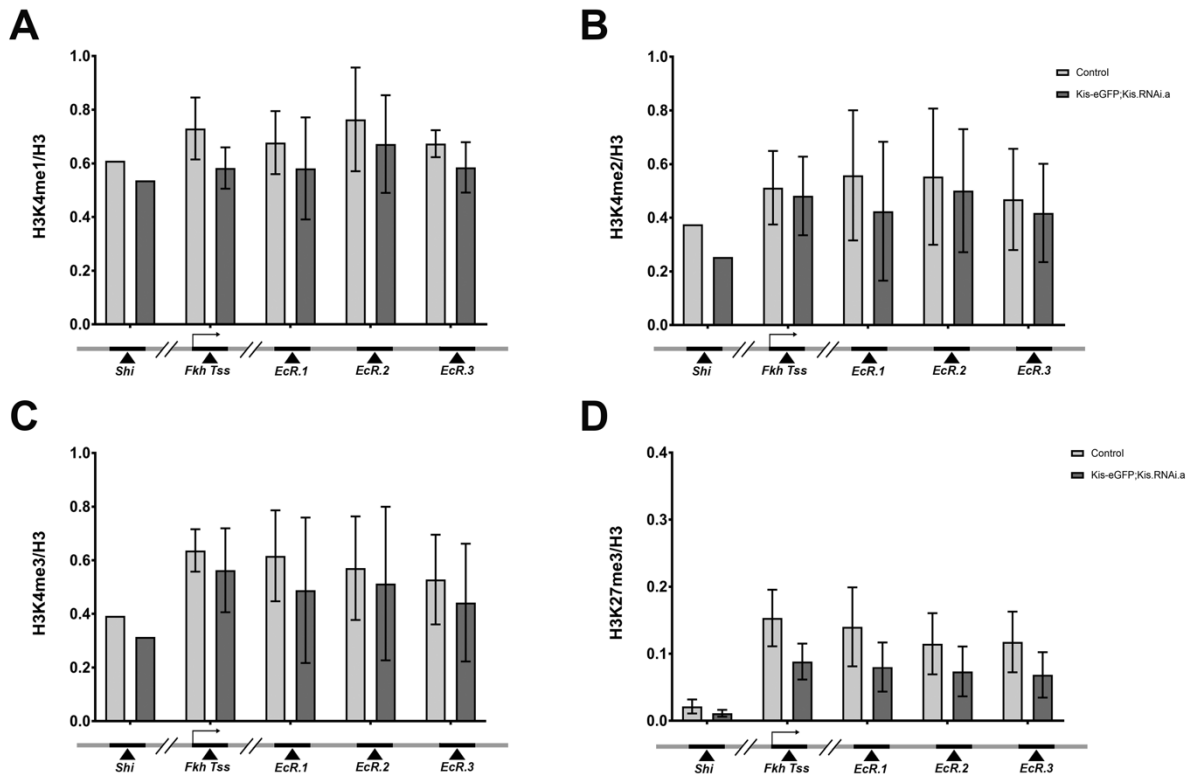
Figure S6. Kis does not alter H3K4 or H3K27 methylation at *EcR* loci, related to Figure 2.
(A-D) ChIP-qPCR analysis of chromatin isolated from brains of control (*Kis-eGFP*) and Kis knockdown (*elav-Gal4; Kis-eGFP/Kis-eGFP; Kis.RNAi.a/+*) 3rd instar larvae. qPCR analysis of H3K4me1 (n = 2 biological replicates), H3K4me2 (n = 2 biological replicates), H3K4me3 (n = 2 biological replicates), H3K27me3 (n = 4 biological replicates) abundance at the *ecr* enhancer sites, the *fkh* TSS, and the *shi* promoter site, respectively. Error bars represent the SEM.
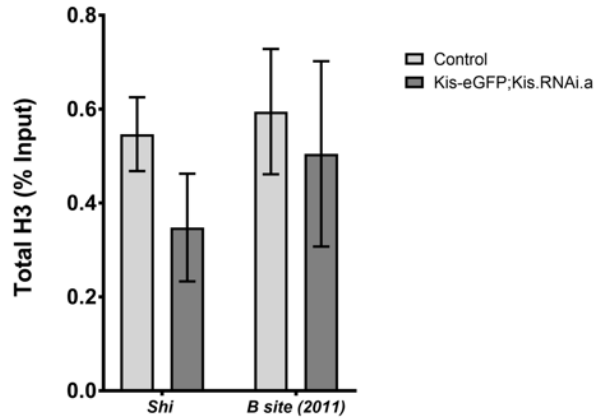
Figure S7. Kis does not alter total histone 3 at *GMR46E06* locus, related to Figure 3. Total H3 as a percentage of the input DNA was determined by qPCR at the previously noted genomic loci using *Kis-eGFP* (control) and *elav-Gal4; Kis-eGFP/Kis-eGFP; Kis.RNAi.a/+* (Kis knockdown) 3rd instar larval brains at the *shi* and the *B site 2011* from Boulanger et al 2011 (Boulanger et al., 2011) (n = 3 biological replicates). Error bars represent the SEM.
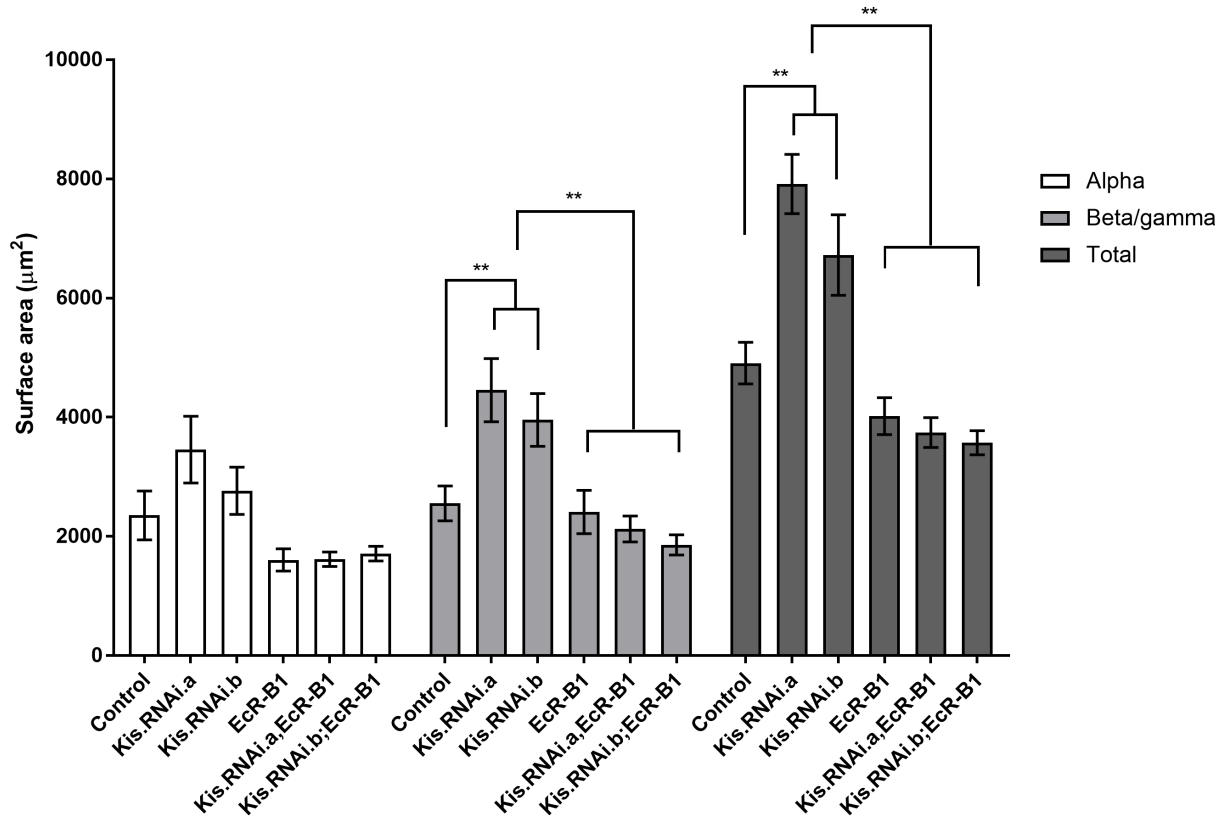
Figure S8. **Transgenic EcR-B1 rescues defective axon pruning in Kis knockdown pupae, related to Figure 4.** Quantification of dorsal, medial, and total MB lobe surface areas in control (*w^1118^*), Kis knockdown (*UAS:Kis.RNAi.a* and *UAS:Kis.RNAi.b*), EcR-B1 overexpression (*UAS:EcR-B1*), and rescue (*UAS:EcR-B1,UAS:Kis.RNAi.a* and *UAS:Kis.RNAi.b; UAS:EcR-B1*) using the *elav-Gal-4,UAS:mCD8-GFP* driver 18-22 hrs APF (n = 9, 9, 8, 7, 10, 11). Statistical significance is represented by ** = p < 0.01. Error bars represent the SEM.
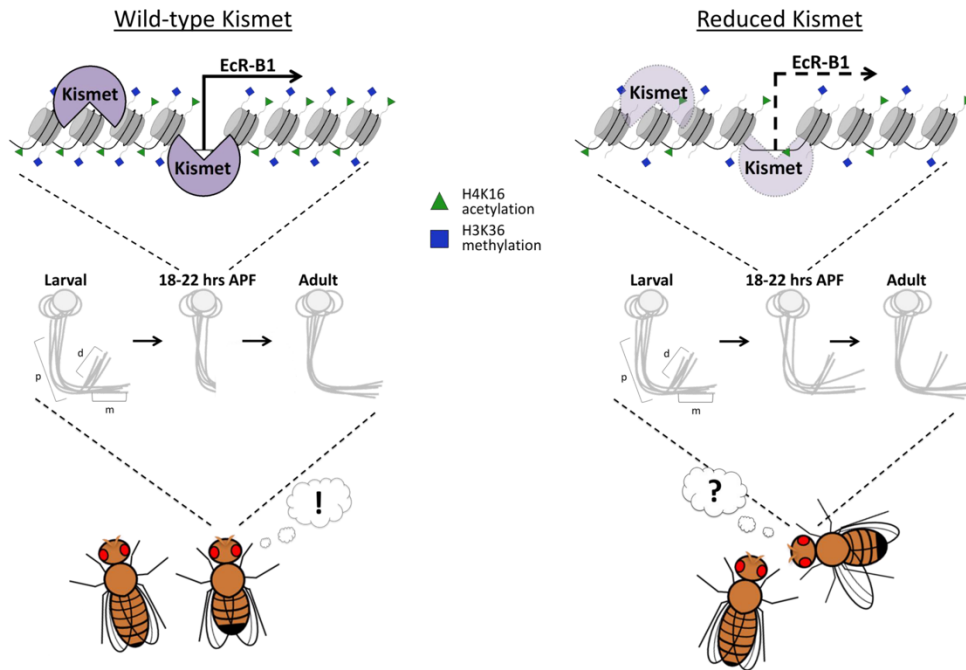
Figure S9. Model of Kis mediated expression of EcR-B1 necessary for MB pruning and behavior, related to Figures 1-7. In wild-type flies, Kis promotes the active H3K36 methylation (blue square) and H4K16 acetylation (green triangle) histone marks and binds to cis-regulatory elements of the ecr locus promoting ecr-b1 transcription, which is required for proper developmental MB axon pruning. In Kis knockdown animals, Kis binding to the ecr locus is reduced, thereby decreasing H3K36 methylation and H4K16 acetylation marks leading to decreased ecr-b1 mRNA and EcR-B1 protein. Further, reduction of Kis also leads to defects in MB pruning and immediate recall memory.

Supplemental Tables

Table S1. Quantitative RT-PCR primer sequences, related to Figure 1 and Figure 6

Gene of Interest	Forward (5' to 3')	Reverse (5' to 3')
kismet	GCTCGCATCATACTTCTTTACTG	TCGTGTTTCCACTATTGCTTCC
ecr-b1	ACT GGC GCA CTA TAT CGA CG	ACATTTTCGCCCGAATCCCT
gal4	GGATGCTCTTCATGGATTTG	CAACATCATTAGCGTCGGTGAG
rp49	CTGCTCATGCAGAACCGC	CTGCTCATGCAGAACCGC

Table S2. Quantitative PCR primer sequences, related to Figure 2 and Figure 3

Gene of Interest	Forward (5' to 3')	Reverse (5' to 3')
fkh TSS	TCGAGCGGACCAGCAGCTAAAG	TGGGGATTTTTGTTGTCTGCCG
EcR.1	CGTGGCTAGATCGTTATTAACTG	CGTATTTCGATGGTAGGGTGTC
EcR.2	GATGTTCGCATACGCGAATACAG	GCAAATTCGCCTCTTTGTTTGTG
EcR.3	CCGTATCCAACATTCACGTAGAG	TGTATTGCCGAATCGTTGTTGTG
shi pro	GAAGTGCCAAAGATCAAGTTTGTC	GAGGAAATCCTGTCGCATCTC

Transparent Methods

Drosophila stocks and genetics

Unless otherwise noted, all crosses were carried out at 25 °C in a 12:12 light:dark cycle at 60% humidity on standard cornmeal-molasses-agar medium. BL numbers refer to Bloomington Stock Center stock numbers (http://flystocks.bio.indiana.edu/bloomhome.htm). VDRC numbers refer to the Vienna Drosophila Resource Center stock numbers (http://stockcenter.vdrc.at/control/main). To drive the expression of transgenes in *Drosophila*, the Gal4/UAS bipartite system was used as previously described (Brand and Perrimon, 1993). *UAS:Kis.RNAi.a* and *UAS:Kis.RNAi.b* constructs were previously described (Melicharek et al., 2010). The kis^{LM27} allele was generated by EMS mutagenesis, as previously described (Melicharek et al., 2008). *UAS:Kis-L* and *Kis-eGFP* stocks were gifts from J. Tamkun, A. Spradling, respectively (Buszczak et al., 2007; Ghosh et al., 2014). The *201y-Gal4* and *Frt40A* MARCM stocks were gifts from L. Luo (Melicharek et al., 2010). The *ecr* putative enhancer site reporter, *GMR46E06-Gal4*, was obtained as described (Pfeiffer et al., 2011; Pfeiffer et al., 2008). Animals utilized in each assay are listed below.

Assessment of axon pruning (MARCM)
  (1) *y⁻,w⁻,hs:Flp,UAS:CD8-GFP; tubP-Gal80,Frt40A,201y-Gal4/CyO*
  (2) *w⁻; Frt40A*
  (3) *w⁻; Kis^{LM27},Frt40A/CyO*
  (4) *w⁻; UAS:Kis-L,Frt 40A/CyO*
  (5) *w⁻; UAS:Kis-L,Kis^{LM27},Frt40A/CyO*
  (6) *w⁻; Frt40A/CyO; UAS:EcR.B1*
  (7) *w-; Kis^{LM27},Frt40A/CyO; UAS:EcR.B1*

EcR-B1 staining and assessment of axon pruning (RNAi)
  (1) *elav-Gal4,UAS:mCD8-GFP* (BL #5146)
  (2) w^{1118} (BL #5905)
  (3) *w⁻; +/+; UAS:Kis.RNAi.a* (VDRC #10762)
  (4) *w⁻; UAS:Kis.RNAi.b* (VDRC #46685)

(5)   *w⁻; UAS:Kis-L*

(6)   *w⁻; UAS:Kis-L; UAS:Kis.RNAi.a*

(7)   *w⁻; UAS:Kis-L,UAS:Kis.RNAi.b*

(8)   *w⁻; +/+; UAS:EcR.B1* (BL #6469)

(9)   *w⁻; +/+; UAS:EcR.B1/UAS:Kis.RNAi.a*

(10) *w⁻; UAS:Kis.RNAi.b; UAS:EcR.B1*

ecr-b1 mRNA quantification

(1)   *elav-Gal4* (BL #458)

(2)   *w¹¹¹⁸*

(3)   *w⁻; +/+; UAS:Kis.RNAi.a*

(4)   *w⁻; UAS:Kis.RNAi.b*

(5)   *w⁻; UAS:Kis-L*

(6)   *w⁻; UAS:Kis-L; UAS:Kis.RNAi.a*

(7)   *w⁻; UAS:Kis-L,UAS:Kis.RNAi.b*

ChIP-qPCR, kis-eGFP validation, MNase protection

(1)   *w⁻; Kis-eGFP*

(2)   *elav-Gal4; Kis-eGFP*

(3)   *w⁻; Kis-eGFP; UAS:Kis.RNAi.a*

Gal4 staining and *gal4* mRNA quantification

(1)   *w⁻; +/+; GMR46E06-Gal4* (BL #48166)

(2)   *w¹¹¹⁸*

(3)   *w⁻; +/+; UAS:Kis.RNAi.a*

(4)   *w⁻; UAS:Kis.RNAi.b*

(5)   *w-; UAS:mCD8-GFP* (BL #5137)

Behavioral testing

(1)   *w⁻,hs:Flp,tubP-Gal80,FRT19A; mCD8-GFP/CyO; ok107-Gal4* (BL #44407)

(2)   *w¹¹¹⁸*

(3)   *w⁻; +/+; UAS:EcR.B1*

(4)   *w⁻; +/+; UAS:Kis.RNAi.a*

(5)   *w⁻; +/+; UAS:EcR.B1/UAS:Kis.RNAi.a*

(6)   Canton S

<u>Pharmacological Treatment</u>

Pharmacological treatment media was prepared as described (Latcheva et al., 2018).

Treated fly media was made using dried instant food (Nutri-Fly Instant, Genesee Scientific) with

water containing 1.6% of 10% w/v tegosept (methyl p-hydroxybenzoate in 95% ethanol) and 0.1%

of DMSO vehicle or 10μM SAHA. *Drosophila* were raised on drug containing food for their entire lifespan.

Immunohistochemistry

Immunohistochemical staining was carried out as previously described (D'Rozario et al., 2016). Unless otherwise noted, dissections were performed on Sylgard-coated plates in phosphate buffer and fixed in 4% paraformaldehyde for 25 minutes. In instances of staining, tissues were washed and permeabilized with 0.5% and then 0.1% TritonX-100 in phosphate buffer (0.5% and 0.1% wash buffers, respectively). Tissue was blocked with 10% normal goat serum (in 0.1% wash buffer) before and after incubation with a primary antibody. Overnight incubations with primary and secondary antibodies were performed. Primary antibodies obtained from the Iowa Developmental Hybridoma Bank include α-EcR-B1 (1:200), α-Gal4 (1:200), and α-FasII (1:200). Fluorescently conjugated goat α-rabbit or goat α-mouse secondary antibodies (1:100, Jackson Immunoresearch Labs). Brains were mounted in Vectashield with DAPI (Vector Laboratories, H-1000) and images were obtained using an Olympus Fluoview 1000 laser scanning confocal microscope. Corrected fluorescence intensity was calculated in ImageJ using the following formula: Intergraded Density of selected area – (selected Area * Mean of background).

MARCM Analysis

Mosaic analysis clones were generated as previously described (Bornstein et al., 2015; Lee and Luo, 1999; Wu and Luo, 2006). A 60-minute heat shock at 37 °C occurred 24 hours after initial egg laying. For pupal MB assessment, white pre-pupae were marked throughout a 4-hour window, were fixed overnight in 2% paraformaldehyde 18-22 hours APF, and then dissected in

phosphate buffer. Pupal MB lobes were visualized via mCD8-GFP and confocal stacks of the dorsal and medial lobes were obtained. In ImageJ, Z-projections of Max Intensity were generated for each lobe and surface area was measured by outlining the mCD8-GFP positive axon bundles. Total lobe surface area was calculated by adding dorsal and medial surface areas together. For adult MB assessment, adults were aged 5 days following eclosion and brains were dissected and fixed in 2% paraformaldehyde. Quantification of the number of aberrant axonal projections was performed by observing MBs in the 3D conformation in ImageJ of mCD8-GFP positive FasII negative projections outside of the dorsal lobe (Bornstein et al., 2015).

Quantitative RT-PCR

10 pupal (approximately 18 hours APF) heads or 50 3rd instar larval brains were dissected in ice-cold phosphate buffer per condition for each biological replicate. These were immediately transferred to RNA Later (Abion) and stored in –80 °C. Isolation of total RNA was done using phenol:chloroform extraction followed by alcohol precipitation for purification. RNA was stored in DEPC water at –80 °C. An adapted version of iTaq™ Universal SYBR® Green One-Step protocol (Bio-Rad) was utilized and samples were run on Bio-Rad C1000 Thermal Cycler CFX96 Real-Time system. Primers were made to *kis, ecr-b1,* and *gal4* mRNAs (IDT). ΔC(t) values were calculated by subtracting the C(t) value of each primer set from C(t) value of *rp49* housekeeping control. Fold change in expression was calculated from ΔΔC(t) values. Each experiment was performed in triplicate with at least three biological replicates.

Chromatin Immunoprecipitation

350 brains from 3rd instar larvae were isolated in ice-cold phosphate buffer per condition for each biological replicate. Brains were transferred to 1X phosphate buffered saline (PBS, Hyclone) and stored at –80 °C. A modified version of truChIP Tissue Chromatin Shearing Kit with SDS Shearing Buffer protocol (Covaris) was used to shear the DNA. Heads were washed twice with 1X PBS and then fixed in Buffer A with 1% methanol-free formaldehyde for 5 minutes at room temperature. Fixing was stopped with Quenching Buffer E followed by incubation for 5 minutes at room temperature. Tissue was pelleted by centrifugation at 4 °C for 5 minutes. Supernatant was removed, and tissue was washed twice with cold 1X PBS. Wash buffer (WB) was removed and tissue was homogenized for 2-3 minutes in 500µL Lysis Buffer (LB) B. Volume was increased to 1mL with LB B followed by incubation on rocker at 4 °C for 20 minutes with 3 second vortex every 10 minutes. Lysed tissue was pelleted and resuspended in WB C. Tissue was washed on rocker for 10 minutes at 4°C at which time it was pelleted, followed by an additional washing with WB C without incubation. Pelleted lysed and washed tissue, largely consisting of nuclei, was resuspended in Covaris SDS Shearing Buffer D. The aggregate of nuclei was incubated with Buffer D for 10 minutes with occasional vortex prior to transfer to a TC 12X12 tube for shearing. Shearing followed the S- and E-Series Shearing recommendations for 10 minutes. 1mL aliquots were stored at –80 °C.

Sheared DNA was confirmed to be within a target range of 100-600 bp fragments. Chromatin was immunoprecipitated using Magna ChIP™ HiSens kit (Millipore). 50uL of sheared chromatin was incubated with antibody-coated Magna ChIP Protein A/G Magnetic Beads for 3 hours. Antibodies against modifications H3K27me3 (rabbit, ab195477), H3K4me1 (rabbit, ab8895), H3K4me2 (rabbit, ab7766), H3K4me3 (rabbit, ab8580), H3K36me2 (rabbit, ab9049), H3K36me3 (rabbit, ab9050), H4K16ac (rabbit, emd millipore 07-329) were used and compared to

Histone H3 (rabbit, ab1791) and Histone H4 (rabbit, ab10158) antibodies, as appropriate. α-GFP (rabbit, ab290) was used to examine Kis abundance and α-IgG (rabbit, ab171870) was utilized as a background control. After elution, samples were incubated with RNaseA (10mg/mL, ThermoScientific) at 37 °C for 30 minutes followed by an incubation with proteinase K (10mg/mL, Millipore) at 57 °C overnight and then inactivate at 75 °C for 15 minutes the next day. Isolated DNA was purified via QIAquick® PCR Purification Kit (Qiagen) and stored at –20 °C.

MNase Protection Assay

350 brains from 3rd instar larvae were dissected in ice-cold phosphate buffer per condition for each biological replicate. Brains were transferred to 1X PBS, and stored at –80 °C. An MNase protection assay was performed using an adapted protocol from (Berson et al., 2017; Chereji et al., 2016). Tissue was homogenized in 500µL of crosslinking buffer (60mM KCl, 15mM NaCl, 4mM MgCl2, 15mM HEPES pH 7.6, 0.5mM DTT, 0.5% Triton X-100, protease inhibitor (100X), 2% formaldehyde) and incubated at room temperature for 15 minutes. Crosslinking was quenched with 50µL of 2.5M of glycine and incubated at room temperature for 5 minutes. Samples were washed twice in crosslinking buffer and twice in D1 buffer (25% glycerol, 5mM Mg Acetate, 50mM Tris pH 8.0, 0.1mM EDTA, 5mM DTT) and resuspended in 1mL of MNase buffer (60mM KCl, 15mM NaCl, 15mM Tris pH 7.4, 0.5mM DTT, 0.25M sucrose, 1.0mM CaCl2). 10units MNase (70196Y, Affymetrix) was added to sample tubes and incubated at 37 °C for 30 minutes. Reaction was quenched with EDTA (final 12.5mM) and SDS (final 0.5%). Samples were equilibrated with NaCl (final 140mM) and incubated with RNaseA (10mg/mL) at 37 °C and then overnight with

proteinase K (10mg/mL) at 65 °C and then 15 minutes at 75 °C the next day. DNA was purified via QIAquick PCR Purification Kit and stored at –20 °C.

Quantitative PCR

Purified DNA was used to prepare PCR reaction mixes according to DyNAmo Flash SYBR Green qPCR Kit (ThermoFisher Scientific). Samples were run using Bio-Rad C1000 Thermal Cycler CFX96 Real-Time system. Primers were made to the EcR.1, EcR.2, and EcR.3 enhancer sites as well as to the B site (Boulanger et al. 2011) of the *ecr locus* (IDT). Additionally, positive and negative control primers were made to the TSS of *fkh* and the *shi* promoter site, respectively (IDT). For control and RNAi knockdown analysis, values were adjusted for input at each primer set and $\Delta\Delta C(t)$ values were calculated by subtracting the adjusted $\Delta C(t)$ value of each primer set from the corresponding $\Delta C(t)$ IgG control. Fold change in expression was calculated from $\Delta\Delta C(t)$ values. Each experiment was performed in triplicate with at least three biological replicates.

Behavioral testing

To evaluate learning and memory, the canonical fly courtship behavior was used as a readout in an associative conditioning assay described by Siegel and Hall (Siegel and Hall, 1979). Virgin male flies (0 to 6 hours following eclosion) were collected in individual food vials and aged 5 days. Similarly, virgin female wild-type flies were collected, transferred to collective food vials, and aged 5 days. 24 hours before assessment, virgin wild-type females were mated individually using wild-type males. These flies were subsequently separated from virgin females. This behavioral test was executed in a separate room kept at 25°C and 50% humidity, recorded using a Sony DCR-SR47 Handycam with Carl Zeiss optics, and illuminated from below using a constant

115V white light transilluminator. Genotypes of each male were blinded on the day of the assay and all fly transfers were performed without anesthesia. Aged male flies were transferred to mating chambers (Aktogen) each containing a portioned-off mated female fly. Flies were allowed to acclimate for 2 minutes before the assay. Training was recorded and commenced for 60 minutes. After, the male fly was transferred to a clean mating chamber containing a portioned-off virgin female fly. After a 2-minute acclimation period, the divider was removed, and immediate recall was recorded for 10 minutes. Shams experienced the same manipulations however these aged males were not exposed to any fly during the training portion. Digital video analysis of the time spent courting was performed using iMovie software (Apple). Courtship indices were calculated by total time observed performing courtship behaviors divided by total time assayed.

Statistical analysis

All statistical analyses were performed using GraphPad Prism (v. 7.03). Significance was determined at the 95% confidence interval. Unpaired student's t-test was used for all experiments, except pupal pruning analysis (utilized two-way ANOVA test) and the learning portion of the associative conditioning assay (utilized paired student's t-test). Statistical significance in figures is represented by $* = p < 0.05$, $** = p < 0.01$, $*** = p < 0.001$, $**** = p < 0.0001$. Error bars represent the standard error of the mean (SEM).

Supplemental References

Berson, A., Sartoris, A., Nativio, R., Van Deerlin, V., Toledo, J.B., Porta, S., Liu, S., Chung, C.Y., Garcia, B.A., Lee, V.M.*, et al.* (2017). TDP-43 Promotes Neurodegeneration by Impairing Chromatin Remodeling. Curr Biol *27*, 3579-3590 e3576.

Bornstein, B., Zahavi, E.E., Gelley, S., Zoosman, M., Yaniv, S.P., Fuchs, O., Porat, Z., Perlson, E., and Schuldiner, O. (2015). Developmental Axon Pruning Requires Destabilization of Cell Adhesion by JNK Signaling. Neuron *88*, 926-940.

Brand, A.H., and Perrimon, N. (1993). Targeted gene expression as a means of altering cell fates and generating dominant phenotypes. Development *118*, 401-415.

Buszczak, M., Paterno, S., Lighthouse, D., Bachman, J., Planck, J., Owen, S., Skora, A.D., Nystul, T.G., Ohlstein, B., Allen, A.*, et al.* (2007). The carnegie protein trap library: a versatile tool for Drosophila developmental studies. Genetics *175*, 1505-1531.

Chereji, R.V., Kan, T.W., Grudniewska, M.K., Romashchenko, A.V., Berezikov, E., Zhimulev, I.F., Guryev, V., Morozov, A.V., and Moshkin, Y.M. (2016). Genome-wide profiling of nucleosome sensitivity and chromatin accessibility in Drosophila melanogaster. Nucleic Acids Res *44*, 1036-1051.

D'Rozario, M., Zhang, T., Waddell, E.A., Zhang, Y., Sahin, C., Sharoni, M., Hu, T., Nayal, M., Kutty, K., Liebl, F.*, et al.* (2016). Type I bHLH Proteins Daughterless and Tcf4 Restrict Neurite Branching and Synapse Formation by Repressing Neurexin in Postmitotic Neurons. Cell reports *15*, 386-397.

Ghosh, R., Vegesna, S., Safi, R., Bao, H., Zhang, B., Marenda, D.R., and Liebl, F.L. (2014). Kismet positively regulates glutamate receptor localization and synaptic transmission at the Drosophila neuromuscular junction. PLoS One *9*, e113494.

Latcheva, N.K., Viveiros, J.M., Waddell, E.A., Nguyen, P.T.T., Liebl, F.L.W., and Marenda, D.R. (2018). Epigenetic crosstalk: Pharmacological inhibition of HDACs can rescue defective synaptic morphology and neurotransmission phenotypes associated with loss of the chromatin reader Kismet. Mol Cell Neurosci *87*, 77-85.

Lee, T., and Luo, L. (1999). Mosaic analysis with a repressible cell marker for studies of gene function in neuronal morphogenesis. Neuron *22*, 451-461.

Melicharek, D., Shah, A., DiStefano, G., Gangemi, A.J., Orapallo, A., Vrailas-Mortimer, A.D., and Marenda, D.R. (2008). Identification of Novel Regulators of Atonal Expression in the Developing Drosophila Retina. Genetics *180*, 2095–2110.

Melicharek, D.J., Ramirez, L.C., Singh, S., Thompson, R., and Marenda, D.R. (2010). Kismet/CHD7 regulates axon morphology, memory and locomotion in a Drosophila model of CHARGE syndrome. Hum Mol Genet *19*, 4253-4264.

Pfeiffer, B.D., Jenett, A., Hammonds, A.S., Ngo, T.T., Misra, S., Murphy, C., Scully, A., Carlson, J.W., Wan, K.H., Laverty, T.R*., et al.* (2011). GAL4 Driver Collection of Rubin Laboratory at Janelia Farm.

Pfeiffer, B.D., Jenett, A., Hammonds, A.S., Ngo, T.T.B., Misra, S., Murphy, C., Scully, A., Carlson, J.W., Wan, K.H., Laverty, T.R*., et al.* (2008). Tools for neuroanatomy and neurogenetics in Drosophila. Proceedings of the National Academy of Sciences of the United States of America *105*, 9715-9720.

Siegel, R.W., and Hall, J.C. (1979). Conditioned responses in courtship behavior of normal and mutant Drosophila. Proc Natl Acad Sci U S A *76*, 3430-3434.

Wu, J.S., and Luo, L. (2006). A protocol for mosaic analysis with a repressible cell marker (MARCM) in Drosophila. Nature protocols *1*, 2583-2589.